Early-Universe Tests of Dark Matter-Baryon Interactions

Tracy Slatyer

MIT

Lawrence Berkeley National Laboratory
Particle Theory Seminar
24 October 2018

Based on work with Chih-Liang Wu (PRD 98, 023013, 1803.09734)
and Mohammad Namjoo & Chih-Liang Wu (1810.09455)

U.S. DEPARTMENT OF ENERGY | Office of Science

Outline

- Tests of dark matter - baryon scattering from the early universe
  - The cosmic microwave background (anisotropies)
  - 21cm line emission
  - The cosmic microwave background (spectrum)
- Indirect searches for n-body dark matter annihilation
  - Parametric estimates
  - Can we see annihilation products from thermal relics?
  - The unitarity bound on velocity-enhanced signals

The puzzle of dark matter

- Roughly 80% of the matter in the universe is DARK - no electric charge, interacts at most very weakly with known particles.
- Multiple lines of evidence for this statement: rotation curves in galaxies, gravitational lensing of colliding galaxy clusters, imprints left on the cosmic microwave background, even the formation of galaxies.
- BUT - has only ever been detected by its gravitational interactions.
- No good candidates in known physics - one of our biggest clues to what might lie beyond the known.

Scattering

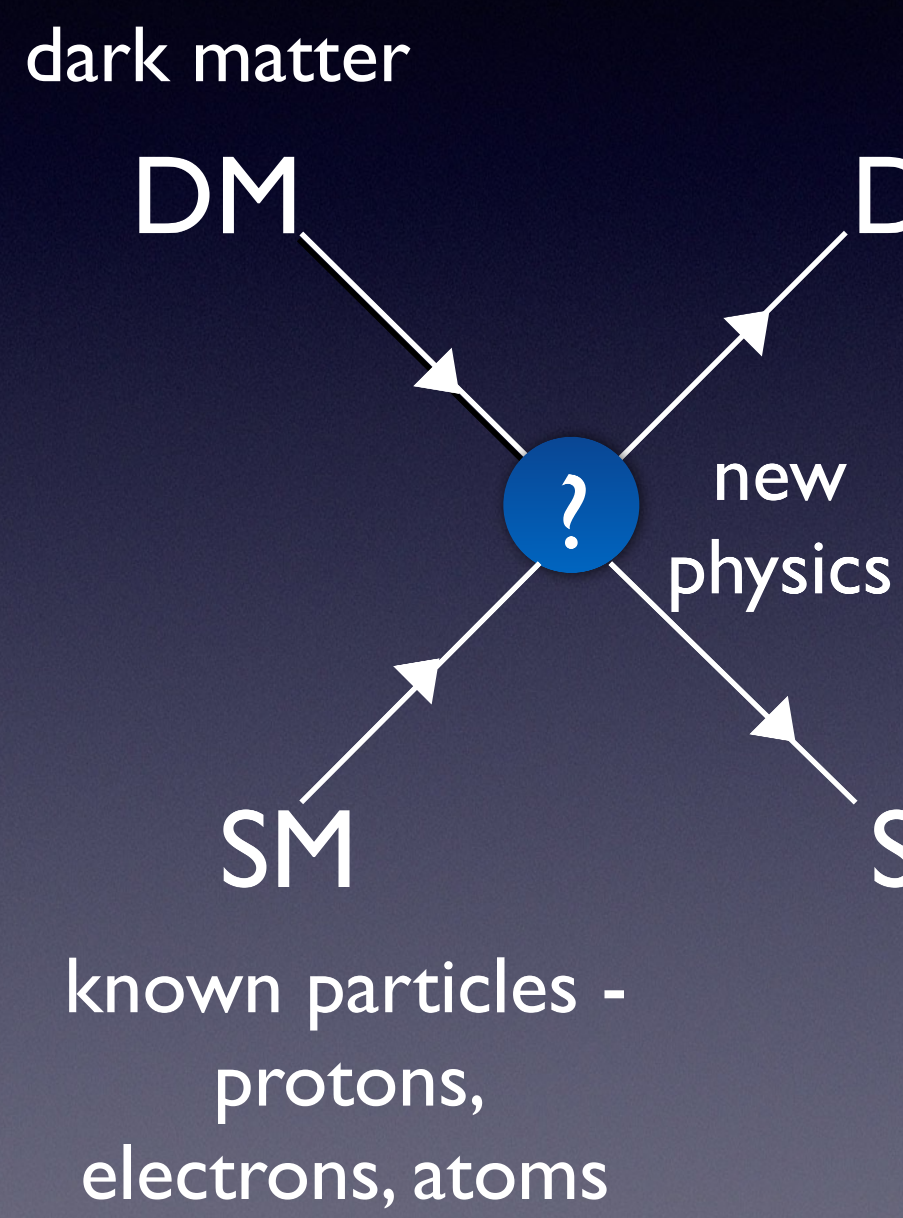

Look for effects of energy transfer to/from DM on visible matter

Direct detection

- Canonical search for GeV-TeV scale DM - look for nuclear recoils from DM-nucleus scattering. But loses sensitivity for DM masses below ~GeV due to kinematics.
- Electron recoil searches work down to ~MeV scales.
- At lower scales, many new ideas in recent years to detect tiny energy transfers.
- Limitations:
  - different mass scales require entirely new experimental techniques
  - signal depends on local DM density/velocity; sufficiently high interaction cross sections may be screened by the Earth/atmosphere

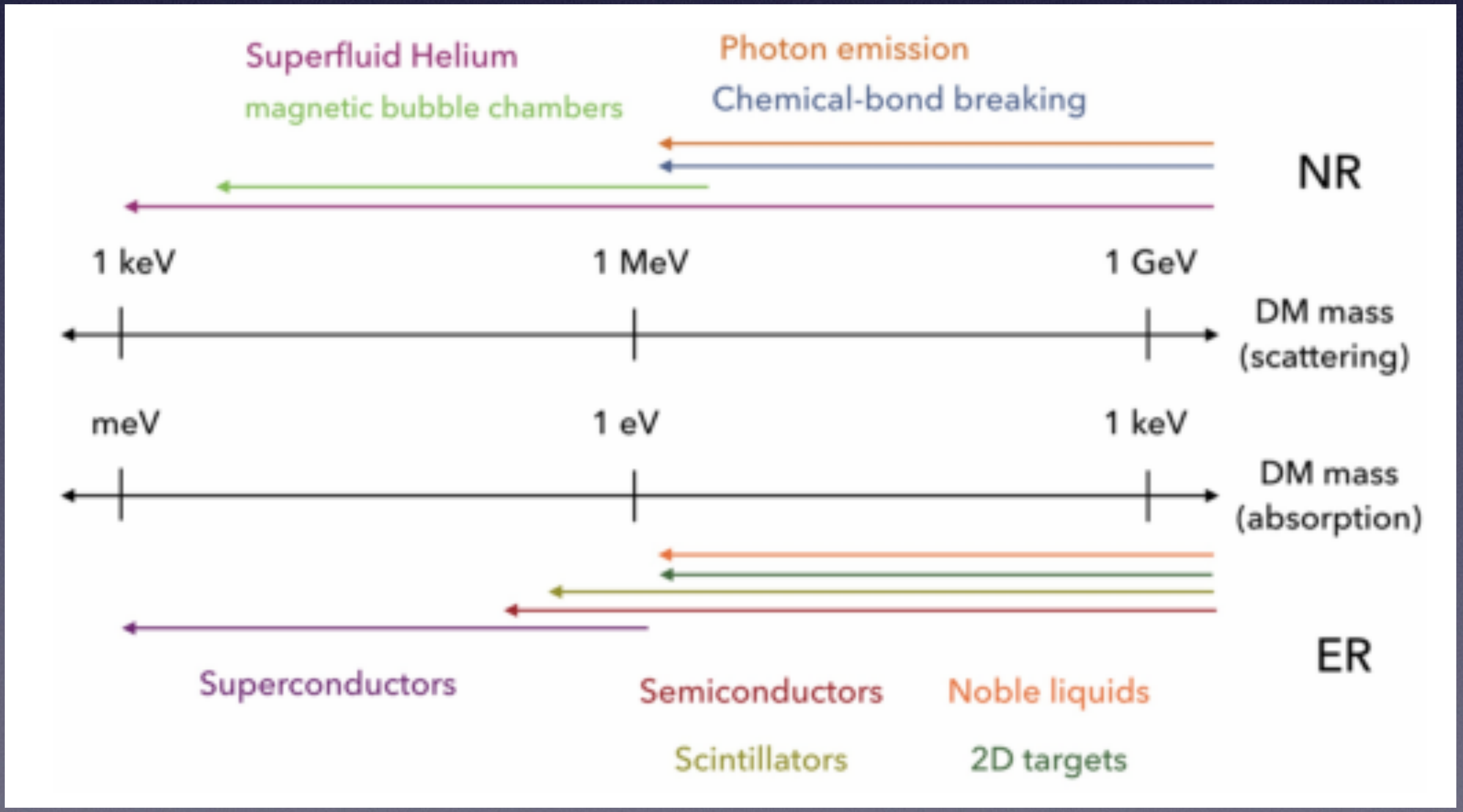

Battaglieri et al, Cosmic Visions '17

The cosmic microwave background

- Emitted at z~1000 (T~few x 0.1 eV) when the universe transitions from 1-ε ionized to 1-ε neutral (“recombination”), path length for photon scattering increases dramatically.
- Typical energy today ~ few x 10^{-4} eV, wavelength ~mm.
- Temperature/polarization anisotropies and energy spectrum are sensitive to behavior of photon-baryon plasma prior to recombination.
- Anisotropies are sensitive to changes to ionization history after recombination (free electrons act as a screen).

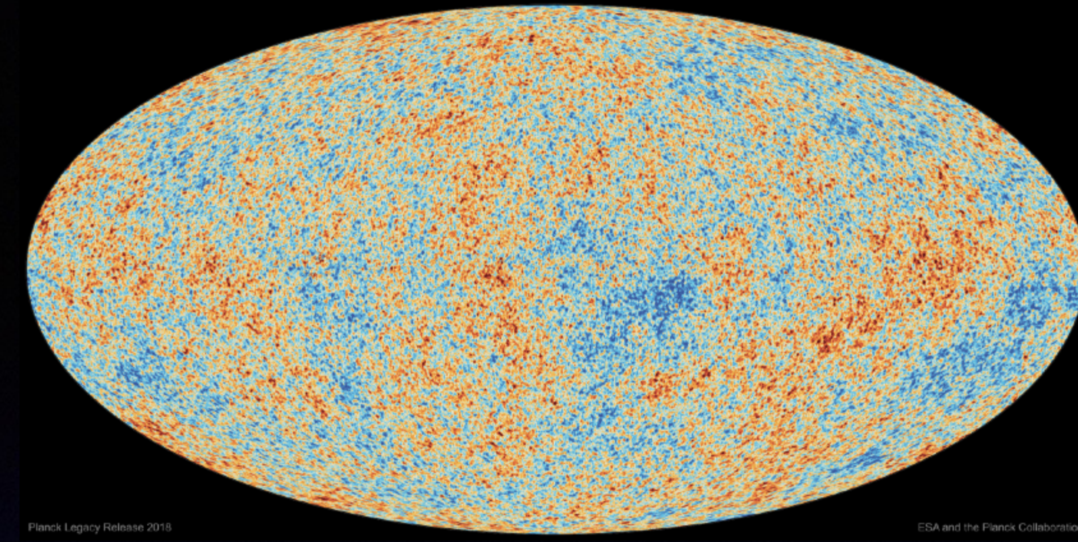

Image credit: European Space Agency / Planck Collaboration

spatial information: describes pattern of oscillations in density and temperature

spectral information: near-perfect blackbody

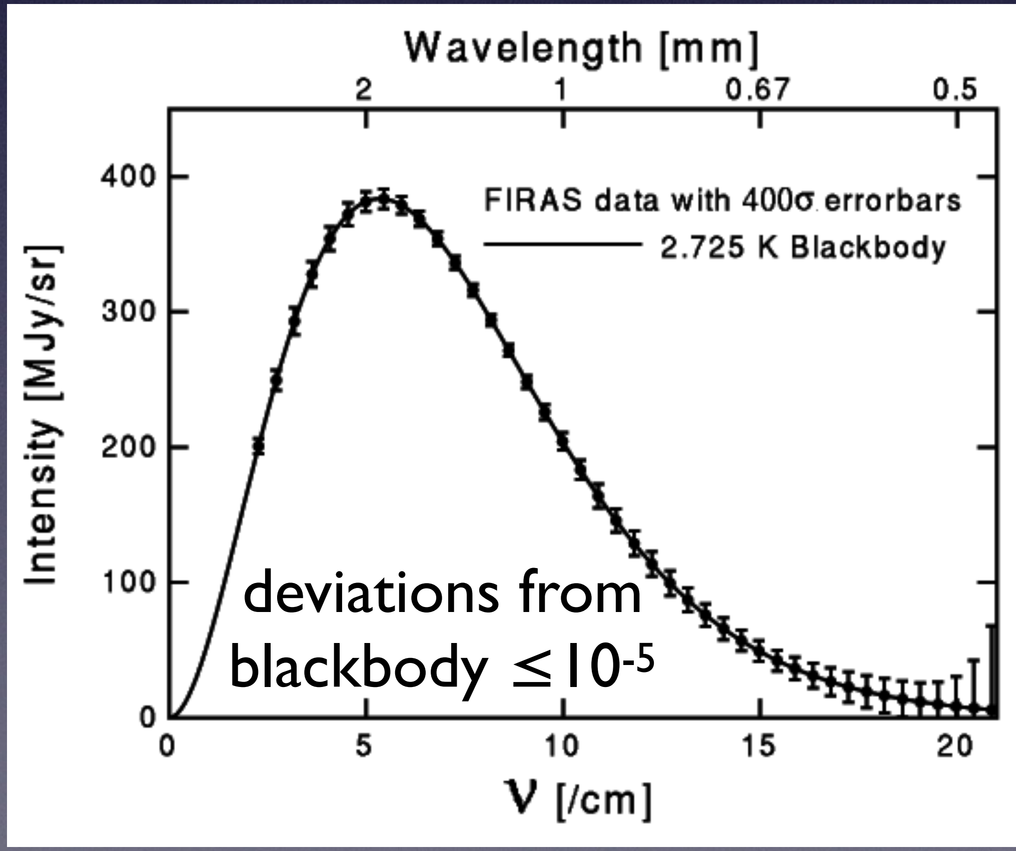

Perturbations in the primordial plasma

- Density/temperature fluctuations in the plasma evolve under gravity and radiation pressure.
- Coupled (linearized) evolution equations describe density and velocity perturbations for baryons, dark matter, photons.
- Separate into different k-modes, study mode evolution.
- Predicts power spectrum of CMB anisotropies - one of the strongest pieces of evidence for dark matter, assuming zero coupling between DM and baryons.

density fluctuations

$$\dot{\delta}_\chi = -\theta_\chi - \frac{\dot{h}}{2},$$

$$\dot{\delta}_b = -\theta_b - \frac{\dot{h}}{2},$$

velocity fluctuations

$$\dot{\theta}_\chi = -\frac{\dot{a}}{a}\theta_\chi + c_\chi^2 k^2 \delta_\chi$$

$$\dot{\theta}_b = -\frac{\dot{a}}{a}\theta_b + c_b^2 k^2 \delta_b + R_\gamma (\theta_\gamma - \theta_b)$$

$$\dot{\theta}_\gamma = k^2 \left(\frac{1}{4}\delta_\gamma - \sigma_\gamma\right) - \frac{1}{\tau_c}(\theta_\gamma - \theta_b). \quad (1)$$

where c_χ and c_b are the sound speeds (for DM/baryons respectively) defined by:

$$c_b^2 = \frac{k_B T_b}{\mu_b}\left(1 - \frac{1}{3}\frac{d\ln T_b}{d\ln a}\right),$$

$$c_\chi^2 = \frac{k_B T_\chi}{m_\chi}\left(1 - \frac{1}{3}\frac{d\ln T_\chi}{d\ln a}\right), \quad (2)$$

$$\mu_b = m_H(n_H + 4n_{He})/(n_H + n_{He} + n_e)$$

Perturbations in the primordial plasma

- Density/temperature fluctuations in the plasma evolve under gravity and radiation pressure.
- Coupled (linearized) evolution equations describe density and velocity perturbations for baryons, dark matter, photons.
- Separate into different k-modes, study mode evolution.
- Predicts power spectrum of CMB anisotropies - one of the strongest pieces of evidence for dark matter, assuming zero coupling between DM and baryons.

coupling to metric perturbations

density fluctuations

$$\dot{\delta}_\chi = -\theta_\chi - \frac{\dot{h}}{2},$$
$$\dot{\delta}_b = -\theta_b - \frac{\dot{h}}{2},$$

velocity fluctuations

$$\dot{\theta}_\chi = -\frac{\dot{a}}{a}\theta_\chi + c_\chi^2 k^2 \delta_\chi$$
$$\dot{\theta}_b = -\frac{\dot{a}}{a}\theta_b + c_b^2 k^2 \delta_b + R_\gamma(\theta_\gamma - \theta_b)$$

$$\dot{\theta}_\gamma = k^2\left(\frac{1}{4}\delta_\gamma - \sigma_\gamma\right) - \frac{1}{\tau_c}(\theta_\gamma - \theta_b). \quad (1)$$

where c_χ and c_b are the sound speeds (for DM/baryons respectively) defined by:

$$c_b^2 = \frac{k_B T_b}{\mu_b}\left(1 - \frac{1}{3}\frac{d\ln T_b}{d\ln a}\right),$$
$$c_\chi^2 = \frac{k_B T_\chi}{m_\chi}\left(1 - \frac{1}{3}\frac{d\ln T_\chi}{d\ln a}\right), \quad (2)$$

$$\mu_b = m_H(n_H + 4n_{He})/(n_H + n_{He} + n_e)$$

Perturbations in the primordial plasma

- Density/temperature fluctuations in the plasma evolve under gravity and radiation pressure.
- Coupled (linearized) evolution equations describe density and velocity perturbations for baryons, dark matter, photons.
- Separate into different k-modes, study mode evolution.
- Predicts power spectrum of CMB anisotropies - one of the strongest pieces of evidence for dark matter, assuming zero coupling between DM and baryons.

coupling to metric perturbations

density fluctuations

$$\dot{\delta}_\chi = -\theta_\chi - \frac{\dot{h}}{2},$$

$$\dot{\delta}_b = -\theta_b - \frac{\dot{h}}{2},$$

velocity fluctuations

$$\dot{\theta}_\chi = -\frac{\dot{a}}{a}\theta_\chi + c_\chi^2 k^2 \delta_\chi$$

$$\dot{\theta}_b = -\frac{\dot{a}}{a}\theta_b + c_b^2 k^2 \delta_b + R_\gamma(\theta_\gamma - \theta_b)$$

shear stress

$$\dot{\theta}_\gamma = k^2\left(\frac{1}{4}\delta_\gamma - \sigma_\gamma\right) - \frac{1}{\tau_c}(\theta_\gamma - \theta_b). \qquad (1)$$

where c_χ and c_b are the sound speeds (for DM/baryons respectively) defined by:

$$c_b^2 = \frac{k_B T_b}{\mu_b}\left(1 - \frac{1}{3}\frac{d\ln T_b}{d\ln a}\right),$$

$$c_\chi^2 = \frac{k_B T_\chi}{m_\chi}\left(1 - \frac{1}{3}\frac{d\ln T_\chi}{d\ln a}\right), \qquad (2)$$

$$\mu_b = m_H(n_H + 4n_{He})/(n_H + n_{He} + n_e)$$

Perturbations in the primordial plasma

- Density/temperature fluctuations in the plasma evolve under gravity and radiation pressure.
- Coupled (linearized) evolution equations describe density and velocity perturbations for baryons, dark matter, photons.
- Separate into different k-modes, study mode evolution.
- Predicts power spectrum of CMB anisotropies - one of the strongest pieces of evidence for dark matter, assuming zero coupling between DM and baryons.

coupling to metric perturbations

density fluctuations

$$\dot{\delta}_\chi = -\theta_\chi - \frac{\dot{h}}{2},$$

$$\dot{\delta}_b = -\theta_b - \frac{\dot{h}}{2},$$

velocity fluctuations

$$\dot{\theta}_\chi = -\frac{\dot{a}}{a}\theta_\chi + c_\chi^2 k^2 \delta_\chi$$

$$\dot{\theta}_b = -\frac{\dot{a}}{a}\theta_b + c_b^2 k^2 \delta_b + R_\gamma(\theta_\gamma - \theta_b)$$

Compton collisions

shear stress

$$\dot{\theta}_\gamma = k^2\left(\frac{1}{4}\delta_\gamma - \sigma_\gamma\right) - \frac{1}{\tau_c}(\theta_\gamma - \theta_b). \quad (1)$$

where c_χ and c_b are the sound speeds (for DM/baryons respectively) defined by:

$$c_b^2 = \frac{k_B T_b}{\mu_b}\left(1 - \frac{1}{3}\frac{d\ln T_b}{d\ln a}\right),$$

$$c_\chi^2 = \frac{k_B T_\chi}{m_\chi}\left(1 - \frac{1}{3}\frac{d\ln T_\chi}{d\ln a}\right), \quad (2)$$

$$\mu_b = m_H(n_H + 4n_{He})/(n_H + n_{He} + n_e)$$

Perturbations in the primordial plasma (plus...)

- Turning on a small baryon-DM coupling modifies the evolution equations [Sigurdson et al '04].
- Size and functional dependence of the coupling R_χ determined by baryon-DM scattering cross section.
- We can evolve these equations using the public CLASS code [Lesgourgues '11], and constrain R_χ using the CMB.

density fluctuations

velocity divergences

DM-baryon scattering

$$
\begin{aligned}
\dot{\delta}_\chi &= -\theta_\chi - \frac{\dot{h}}{2}, \\
\dot{\delta}_b &= -\theta_b - \frac{\dot{h}}{2}, \\
\dot{\theta}_\chi &= -\frac{\dot{a}}{a}\theta_\chi + c_\chi^2 k^2 \delta_\chi + R_\chi\left(\theta_b - \theta_\chi\right), \\
\dot{\theta}_b &= -\frac{\dot{a}}{a}\theta_b + c_b^2 k^2 \delta_b + R_\gamma\left(\theta_\gamma - \theta_b\right) \\
&\quad + \frac{\rho_\chi}{\rho_b} R_\chi\left(\theta_\chi - \theta_b\right), \\
\dot{\theta}_\gamma &= k^2\left(\frac{1}{4}\delta_\gamma - \sigma_\gamma\right) - \frac{1}{\tau_c}(\theta_\gamma - \theta_b). \qquad (1)
\end{aligned}
$$

where c_χ and c_b are the sound speeds (for DM/baryons respectively) defined by:

$$
\begin{aligned}
c_b^2 &= \frac{k_B T_b}{\mu_b}\left(1 - \frac{1}{3}\frac{d\ln T_b}{d\ln a}\right), \\
c_\chi^2 &= \frac{k_B T_\chi}{m_\chi}\left(1 - \frac{1}{3}\frac{d\ln T_\chi}{d\ln a}\right), \qquad (2)
\end{aligned}
$$

$$\mu_b = m_H(n_H + 4n_{He})/(n_H + n_{He} + n_e)$$

Examples for σ∝vⁿ

- Including only thermal velocities, integrate over (assumed Maxwell-Boltzmann) velocity distributions to get rate coefficient [e.g. Xu et al '18].
- Note: this fails for $z < 10^4$, as there is a non-zero bulk velocity between dark matter and baryons.
- Full treatment of this bulk velocity is very complicated - depends on integral over all momentum modes, couples equations for different k together through R_χ.
- We use the simplified treatment of Dvorkin et al '14; recent in-depth analysis by Boddy et al '18 (1808.00001) finds this is quite a good approximation.

correction due to helium
(=1-Y_{He} = 0.76 if no scattering on helium included

$$R_\chi = \frac{a c_n \rho_b \sigma_0}{m_\chi + m_H} \left(\frac{T_b}{m_H} + \frac{T_\chi}{m_\chi} \right)^{\frac{n+1}{2}} F_{\mathrm{He}},$$

where the numerical prefactor c_n is given by:

$$c_n = \frac{2^{\frac{n+5}{2}} \Gamma\left(3 + \frac{n}{2}\right)}{3\sqrt{\pi}}.$$

$$R_\chi \to \frac{a c_n \rho_b \sigma_0}{m_\chi + m_H} \left(\frac{T_b}{m_H} + \frac{T_\chi}{m_\chi} + \frac{V_{\mathrm{rms}}^2}{3} \right)^{\frac{n+1}{2}} F_{\mathrm{He}},$$

where V_{rms} is estimated as:

$$V_{\mathrm{rms}}^2 \approx \begin{cases} 10^{-8} & z > 10^3 \\ 10^{-8} \left(\frac{1+z}{10^3} \right)^2 & z \leq 10^3. \end{cases}$$

Including temperature evolution

- Temperature enters into evolution equations via the sound speeds [Dvorkin et al '14].
- If n≠-1, rate coefficient also depends on temperature.
- Need to self-consistently solve for temperature evolution to get correct evolution of perturbations.
- Modifying temperature at early times (pre-recombination) also distorts CMB <u>energy</u> spectrum.
- Modifying temperature at late times is an observable in its own right.

$$
\begin{aligned}
\dot{T}_\chi &= -2\frac{\dot{a}}{a}T_\chi + \frac{2m_\chi}{m_\chi + m_H} R_\chi \left(T_b - T_\chi\right), \\
\dot{T}_b &= -2\frac{\dot{a}}{a}T_b + 2\frac{\mu_b}{m_e} R_\gamma \left(T_\gamma - T_b\right) \\
&\quad + \frac{2\mu_b}{m_\chi + m_H}\frac{\rho_\chi}{\rho_b} R_\chi \left(T_\chi - T_b\right).
\end{aligned}
$$

<u>Note</u>: these equations only consider thermal heat transfer, not frictional effects due to DM-baryon bulk velocity. However this effect is subdominant for sub-GeV DM [see Munoz et al '15 for details].

Including temperature evolution

- Temperature enters into evolution equations via the sound speeds [Dvorkin et al '14].
- If n≠-1, rate coefficient also depends on temperature.
- Need to self-consistently solve for temperature evolution to get correct evolution of perturbations.
- Modifying temperature at early times (pre-recombination) also distorts CMB <u>energy</u> spectrum.
- Modifying temperature at late times is an observable in its own right.

cosmological expansion

$$\dot{T}_\chi = -2\frac{\dot{a}}{a}T_\chi + \frac{2m_\chi}{m_\chi + m_H} R_\chi \left(T_b - T_\chi\right),$$

$$\dot{T}_b = -2\frac{\dot{a}}{a}T_b + 2\frac{\mu_b}{m_e} R_\gamma \left(T_\gamma - T_b\right) + \frac{2\mu_b}{m_\chi + m_H}\frac{\rho_\chi}{\rho_b} R_\chi \left(T_\chi - T_b\right).$$

<u>Note</u>: these equations only consider thermal heat transfer, not frictional effects due to DM-baryon bulk velocity. However this effect is subdominant for sub-GeV DM [see Munoz et al '15 for details].

Including temperature evolution

- Temperature enters into evolution equations via the sound speeds [Dvorkin et al ’14].
- If n≠-1, rate coefficient also depends on temperature.
- Need to self-consistently solve for temperature evolution to get correct evolution of perturbations.
- Modifying temperature at early times (pre-recombination) also distorts CMB <u>energy</u> spectrum.
- Modifying temperature at late times is an observable in its own right.

cosmological expansion

$$\dot{T}_\chi = -2\frac{\dot{a}}{a}T_\chi + \frac{2m_\chi}{m_\chi + m_H}R_\chi\left(T_b - T_\chi\right),$$

$$\dot{T}_b = -2\frac{\dot{a}}{a}T_b + 2\frac{\mu_b}{m_e}R_\gamma\left(T_\gamma - T_b\right) + \frac{2\mu_b}{m_\chi + m_H}\frac{\rho_\chi}{\rho_b}R_\chi\left(T_\chi - T_b\right).$$

heating of baryons by CMB

<u>Note</u>: these equations only consider thermal heat transfer, not frictional effects due to DM-baryon bulk velocity. However this effect is subdominant for sub-GeV DM [see Munoz et al ’15 for details].

Including temperature evolution

- Temperature enters into evolution equations via the sound speeds [Dvorkin et al '14].
- If n≠-1, rate coefficient also depends on temperature.
- Need to self-consistently solve for temperature evolution to get correct evolution of perturbations.
- Modifying temperature at early times (pre-recombination) also distorts CMB <u>energy</u> spectrum.
- Modifying temperature at late times is an observable in its own right.

cosmological expansion

$$\dot{T}_\chi = -2\frac{\dot{a}}{a}T_\chi + \frac{2m_\chi}{m_\chi + m_H}R_\chi\left(T_b - T_\chi\right),$$

$$\dot{T}_b = -2\frac{\dot{a}}{a}T_b + 2\frac{\mu_b}{m_e}R_\gamma\left(T_\gamma - T_b\right) + \frac{2\mu_b}{m_\chi + m_H}\frac{\rho_\chi}{\rho_b}R_\chi\left(T_\chi - T_b\right).$$

heating of baryons by CMB

transfer of heat between baryons and DM

<u>Note</u>: these equations only consider thermal heat transfer, not frictional effects due to DM-baryon bulk velocity. However this effect is subdominant for sub-GeV DM [see Munoz et al '15 for details].

Constraints from the CMB

- Modify CLASS to solve new evolution for fixed n.
- Use MontePython + (2015) Planck likelihoods to determine limit on normalization of R_χ
- Note: earlier work studied n=0 [Dvorkin et al '14, Gluscevic & Boddy '18] and n > 0 [Boddy & Gluscevic '18]; n < 0 also studied by Xu et al '18 (v1 had error in n=-4 case; corrected v2 matches our result).

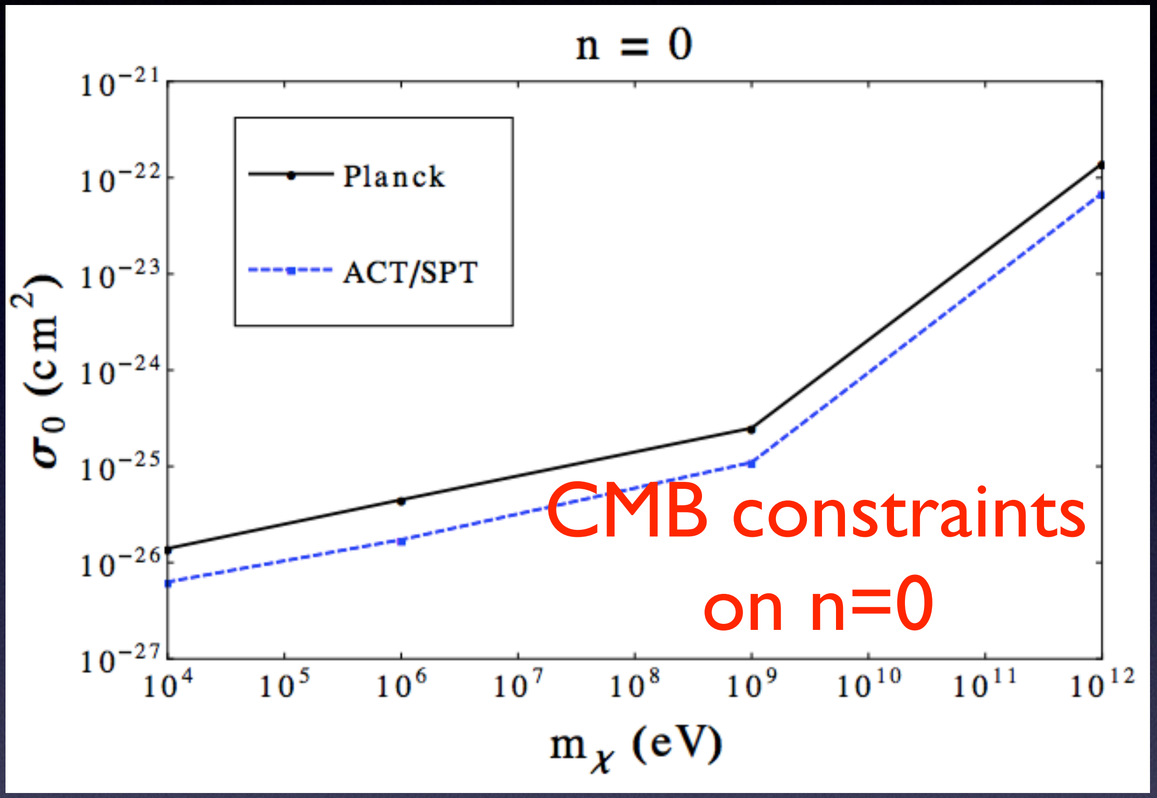

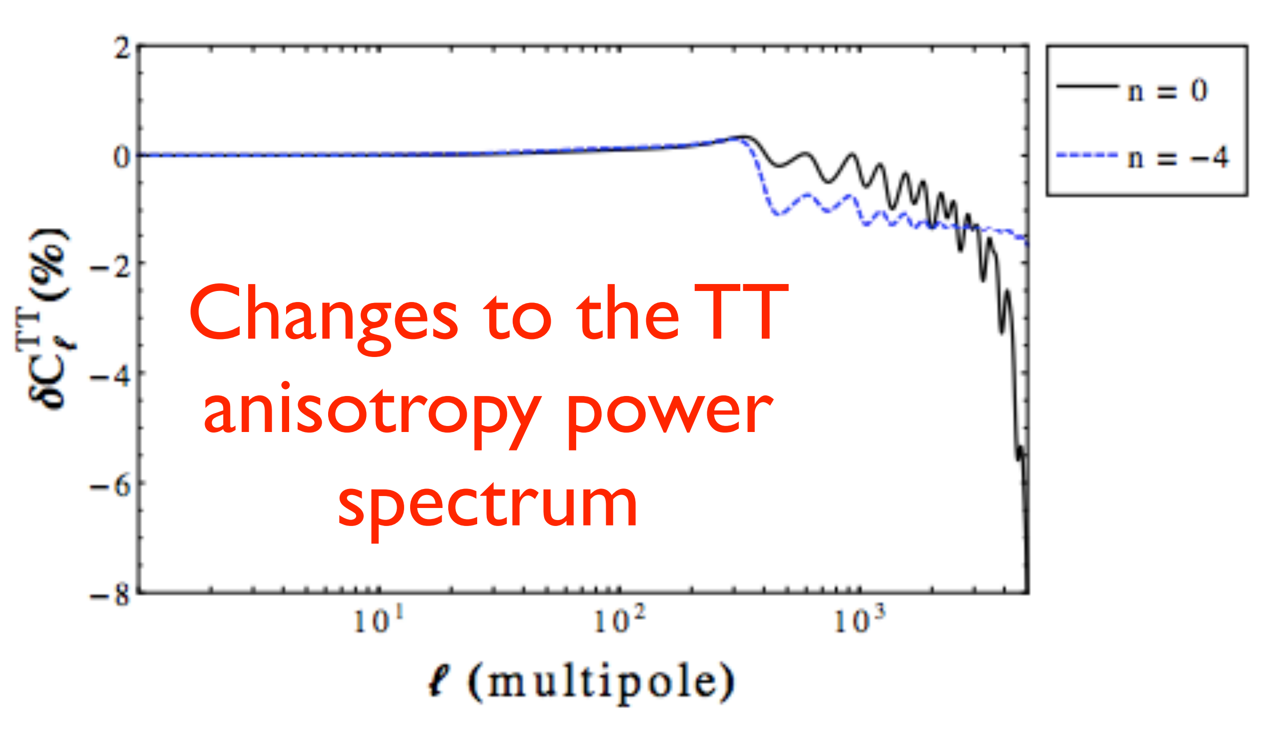

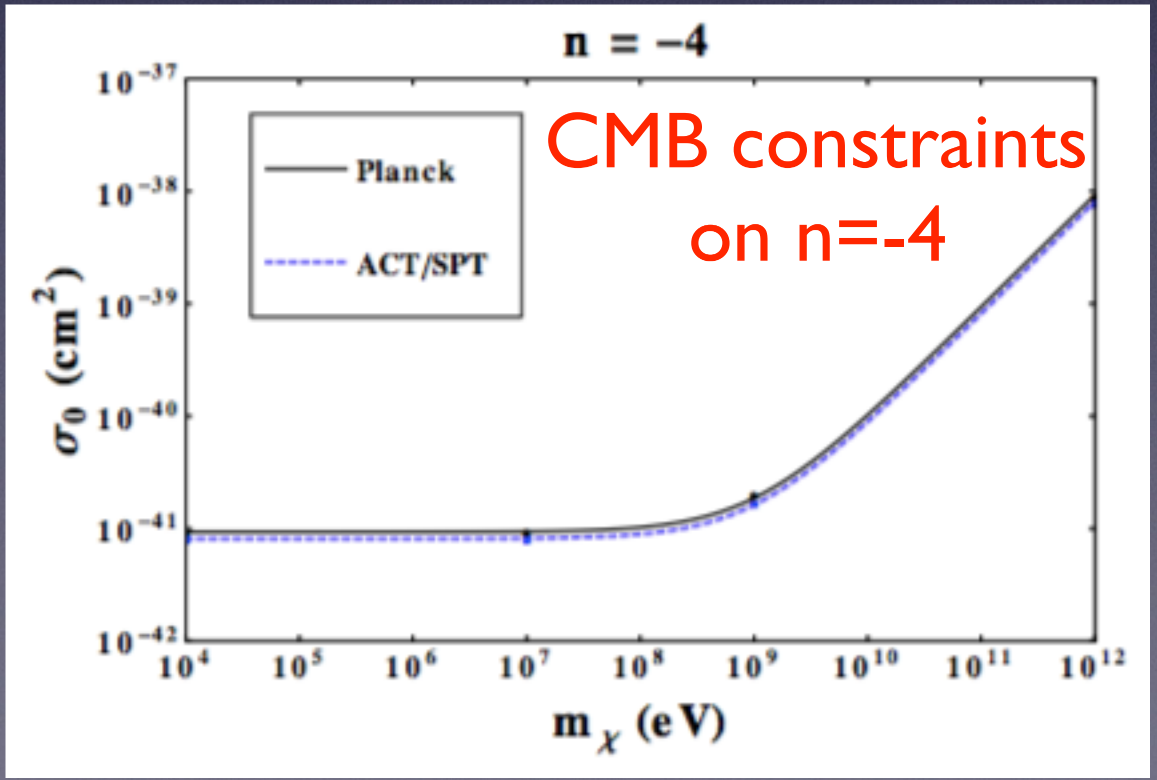

Fisher forecasting

- Markov chain Monte Carlo runs are time-consuming and computationally expensive - but sensitivity of CMB limits, in the absence of a signal, can be estimated more simply

$$\Sigma_\ell = \frac{2}{2l+1}\times \begin{pmatrix} (C_\ell^{TT})^2 & (C_\ell^{TE})^2 & C_\ell^{TT}C_\ell^{TE} \\ (C_\ell^{TE})^2 & (C_\ell^{EE})^2 & C_\ell^{EE}C_\ell^{TE} \\ C_\ell^{TT}C_\ell^{TE} & C_\ell^{EE}C_\ell^{TE} & \frac{1}{2}\left[(C_\ell^{TE})^2 + C_\ell^{TT}C_\ell^{EE}\right] \end{pmatrix}$$

+adjustments for noise & sky coverage

- Covariance between C_l's is known analytically for perfect experiment; experimental noise can be approximately included in a simple way [e.g. Verde '10].

$$C_\ell^{TT,EE} \to C_\ell^{TT,EE} + N_\ell^{TT,EE}$$

$$N_\ell^{TT,EE} = (\Delta T \times \mathrm{FWHM})^2 e^{l(l+1)\theta^2}$$

- Detectability of given signals, covariance between two signals, can be estimated from the Fisher matrix (α_i parameters control strength of different signals, e.g. R_X.)

$$(F_e)_{ij} = \sum_\ell \left(\frac{\partial C_\ell}{\partial \alpha_i}\right)^T \cdot \Sigma_\ell^{-1} \cdot \frac{\partial C_\ell}{\partial \alpha_j}.$$

Linearity

- Fisher matrix is defined by derivatives evaluated at some chosen values for the coefficients.
- Obvious evaluation point is the ΛCDM baseline, $R_X = 0$.
- If the problem is linear, finite signals can be trivially constructed from derivatives at $R_X = 0$.
- Consequently, so long as linearity holds, Fisher matrix describes detectability of arbitrarily large signals.
- So is the problem linear?

Test: examine change in δC_l with increasing xsec

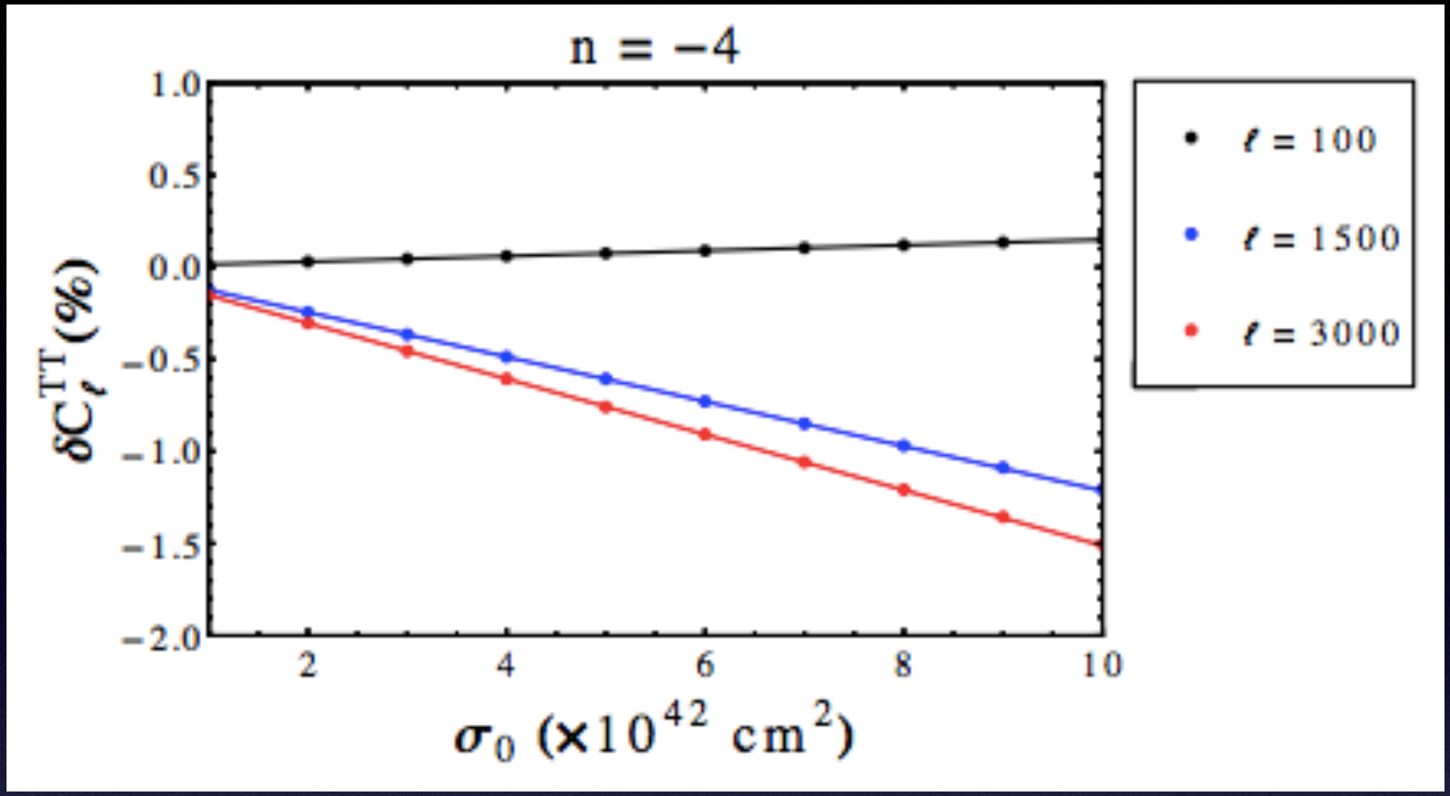

Test: examine change in δC_l due to scattering turned on for a limited time at two different redshifts, compare sum of signals to signal from sum

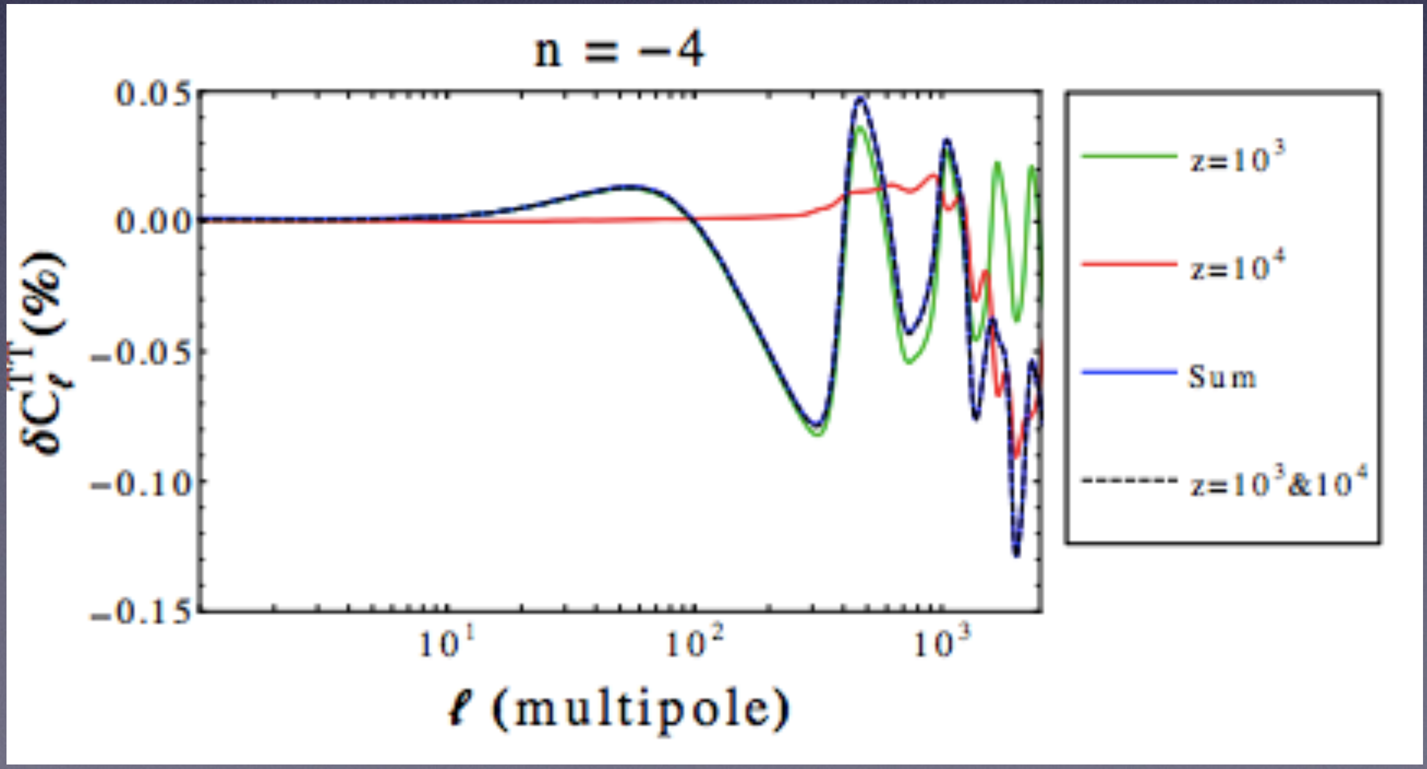

Linearity

- Fisher matrix is defined by derivatives evaluated at some chosen values for the coefficients.
- Obvious evaluation point is the ΛCDM baseline, $R_X = 0$.
- If the problem is linear, finite signals can be trivially constructed from derivatives at $R_X = 0$.
- Consequently, so long as linearity holds, Fisher matrix describes detectability of arbitrarily large signals.
- So is the problem linear? ~yes

Test: examine change in δC_l with increasing xsec

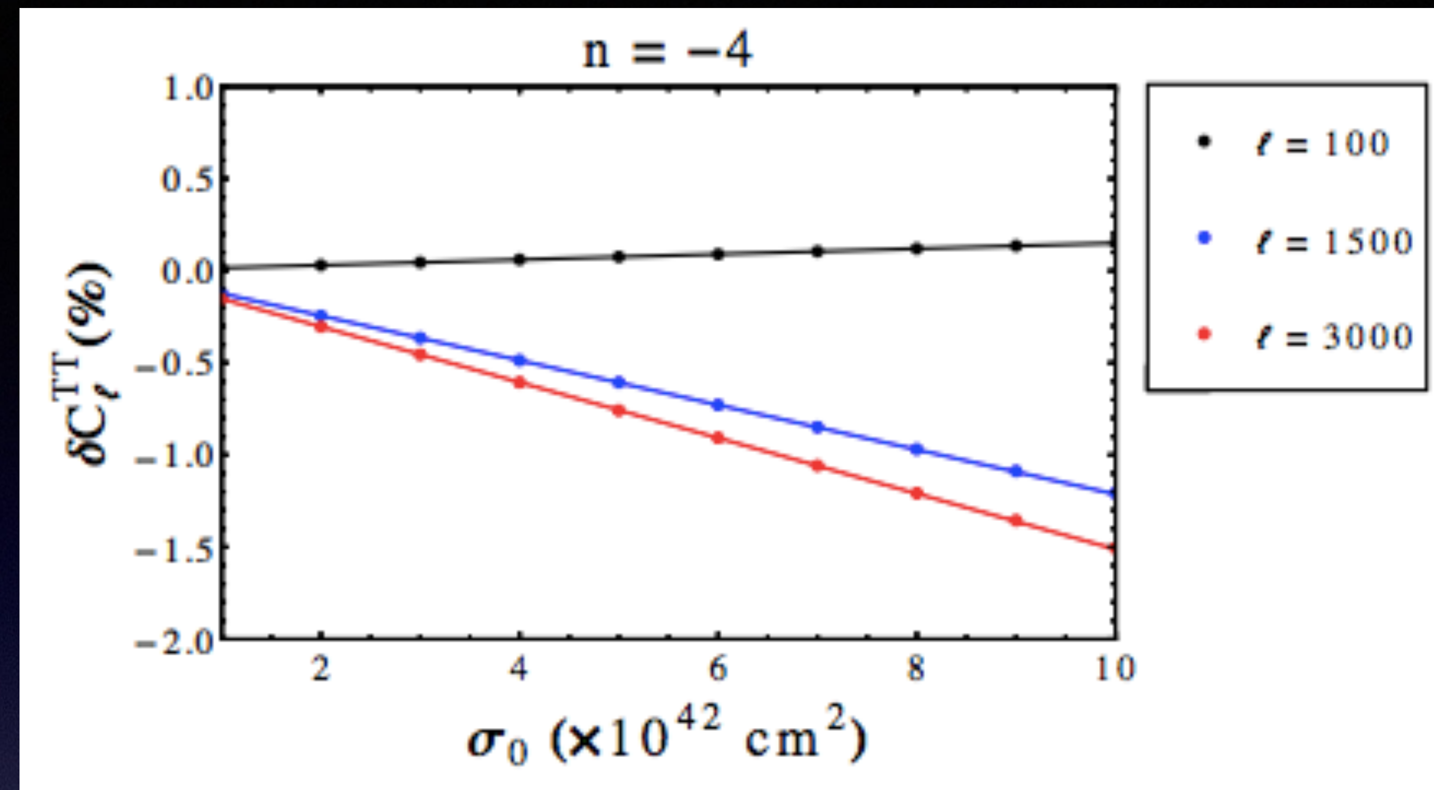

Test: examine change in δC_l due to scattering turned on for a limited time at two different redshifts, compare sum of signals to signal from sum

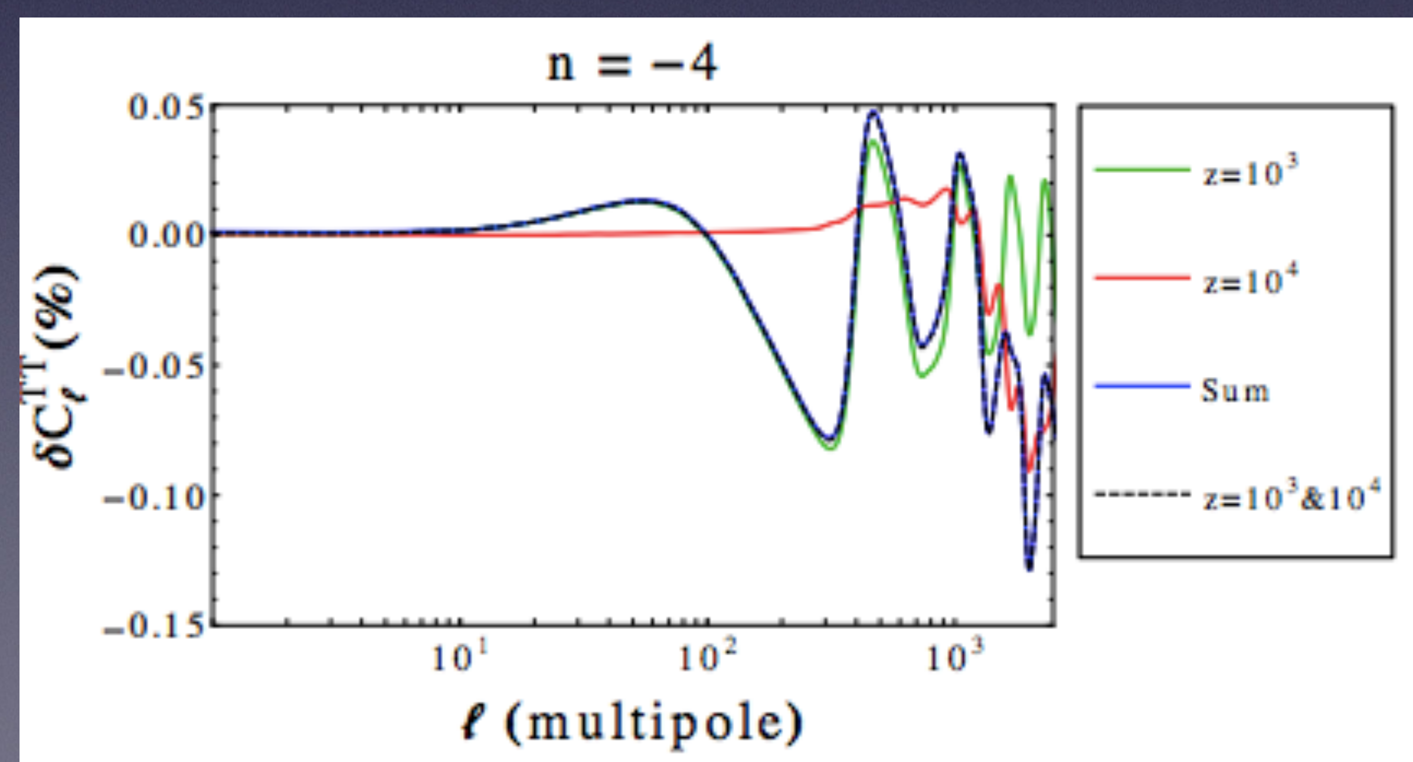

CMB constraints on scattering by redshift

- To understand which redshifts drive the signal, consider the effects of turning on scattering for short periods. In linear regime, can decompose any scattering history this way.
- Generate a Fisher matrix F based on N such basis models, with scattering turned on around redshift z_i, i=1..N.
- Plot F_{ii} to estimate which redshifts have a large signal in the CMB (with parameters z_i,. set by the cross section for that period).
- We see the constraint dominantly comes from z~10^3-few x 10^4 - suppressing signal at these redshifts would evade CMB limits.
- This is determined by the sensitivity of CMB experiments to modes of varying l.

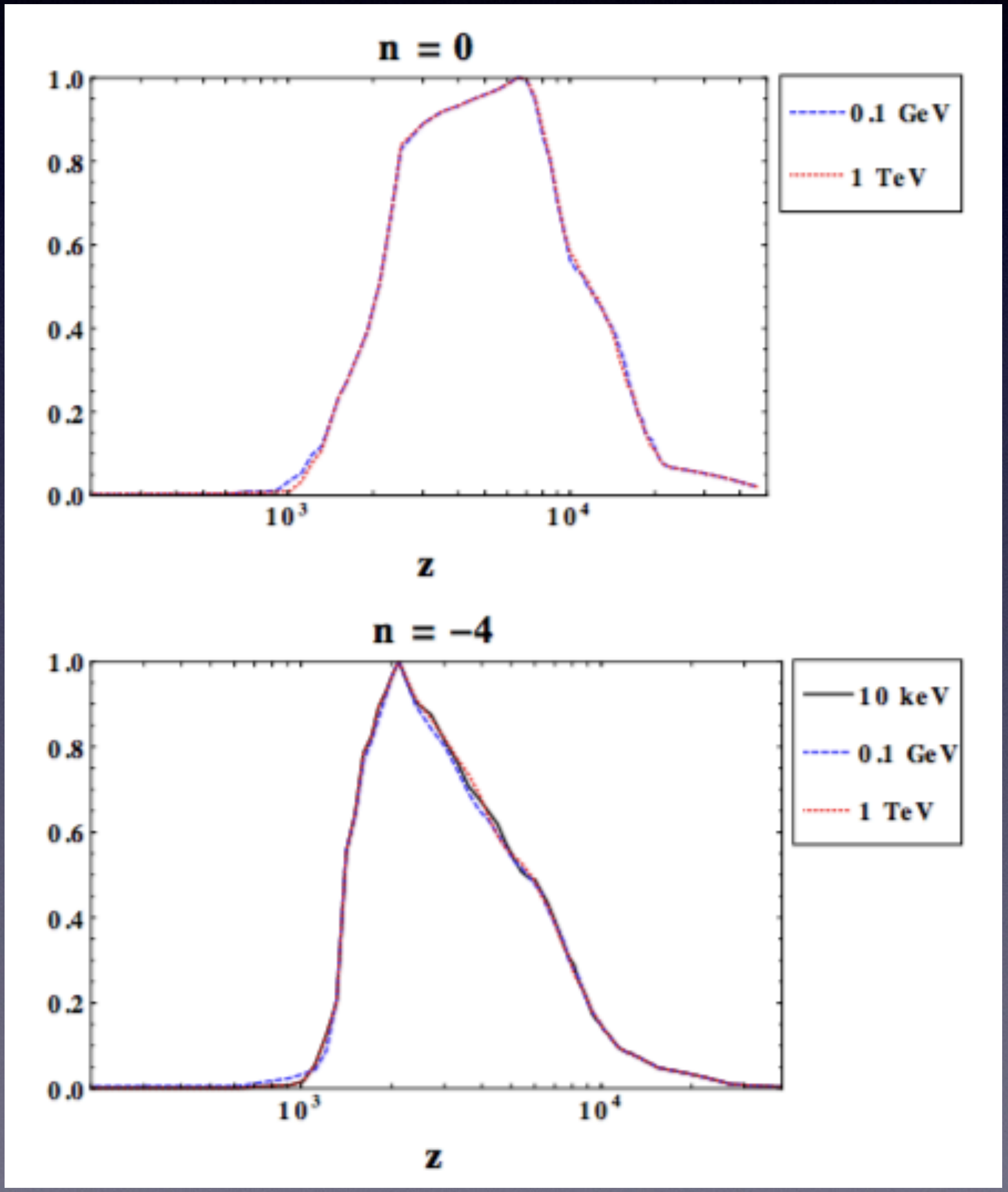

Principal component analysis

- Consider a space of models that span some interesting "model space" and predict signals in some dataset (here, the C_l's of the CMB).
- Model space can generally be very high-dimensional, but signal space may be approximated by a low-dimensional space.
- Goal: find orthogonal basis for signal space, where first few basis vectors capture most of the significance of signals (with respect to some null hypothesis).
- Can then expand any model (within space spanned by initial set) in terms of corresponding model-space basis, and the first few terms in the expansion should largely describe the signal significance.
- Specific example here: we want to decompose general redshift-dependent scattering histories into a simple basis of histories ranked by effect on the CMB.

Toy example

Image credit: http://setosa.io/ev/principal-component-analysis/

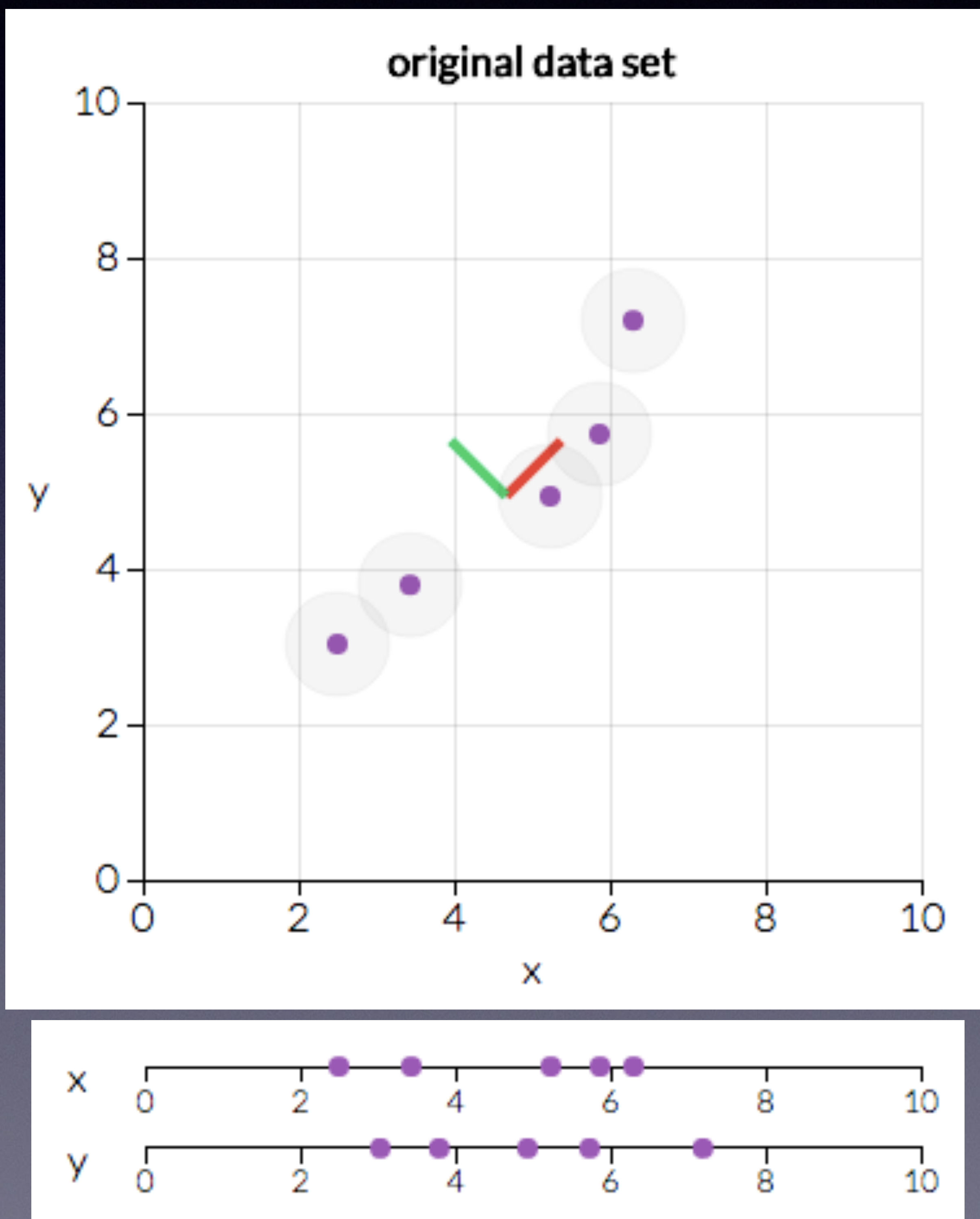

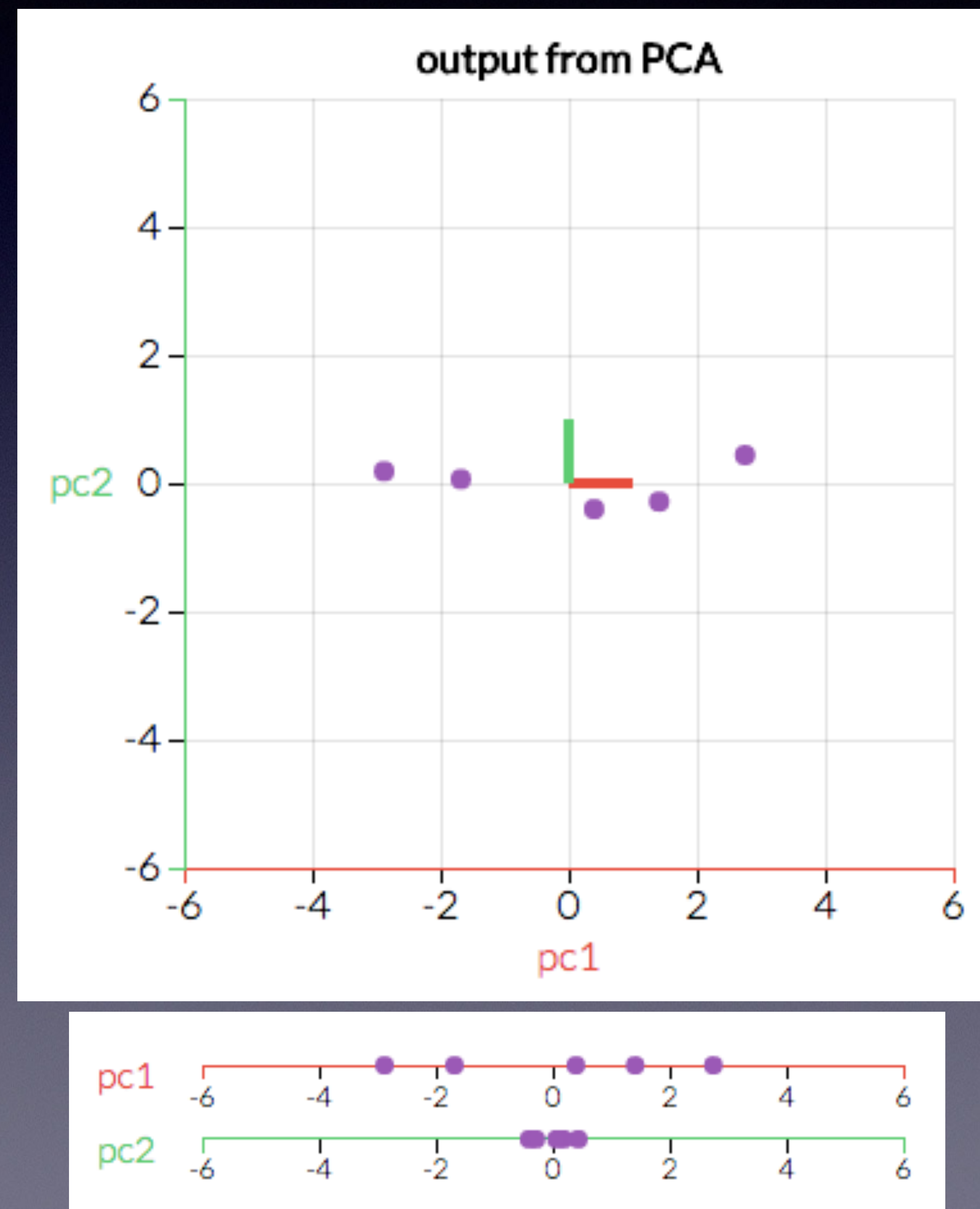

Principal component analysis details

- Calculate Fisher matrix as previously, as a function of model parameters $\{\alpha_i\}$ describing scattering cross section in different cases.
- Marginalize over cosmological parameters by including them in Fisher matrix, then inverting + truncating Fisher matrix.
- Diagonalize this matrix to obtain principal components (eigenvectors) PC_i.
- Eigenvalues λ_i describe the contribution of the corresponding eigenvectors to the variance. Suppose the null hypothesis is the best-fit result, then if a model to be tested can be written in the form

$$\sum \alpha_i \mathrm{PC}_i$$

we estimate it will be excluded with approximately, $\Delta\chi^2 \approx \sum \lambda_i \alpha_i^2$

A redshift-based principal component analysis for DM-baryon scattering

- Basis histories = unit-normalized Gaussian "modulation functions" localized at the centers of redshift bins, $G_i(z)$, multiplying "baseline" history (fixed n).
- The principal components, $P_j(z)$, are dimensionless linear combinations of these $G_i(z)$; to get to corresponding scattering history $\sigma(z)$, multiply $P_j(z)$ by baseline history.
- We find that the first four PCs account for 90-95% of the variance for baselines with n=0 and n=-4.
- Coefficients α_{ij} provided as .dat files with our paper.
- Allows quick estimate of constraints for a wide range of redshift-dependent scattering histories.

$$\sigma(z) \approx \sum_i \sigma(z_i) G_i(z) \approx \frac{\sigma(z_i)}{\sigma_0 v(z_i)^n} \sigma_0 v(z)^n G_i(z)$$

$$G_i(z) = \sum_{j=1}^{N} \alpha_{ij} P_j(z)$$

Eigenvalues

	$n=0$	$n=-4$
σ_0 (cm^2)	10^{-26}	10^{-42}
$\lambda_1 \times 100$	9.8	7.8
$\lambda_2 \times 100$	7.4	6.4
$\lambda_3 \times 100$	2.1	3.2
$\lambda_4 \times 100$	1.6	1.8

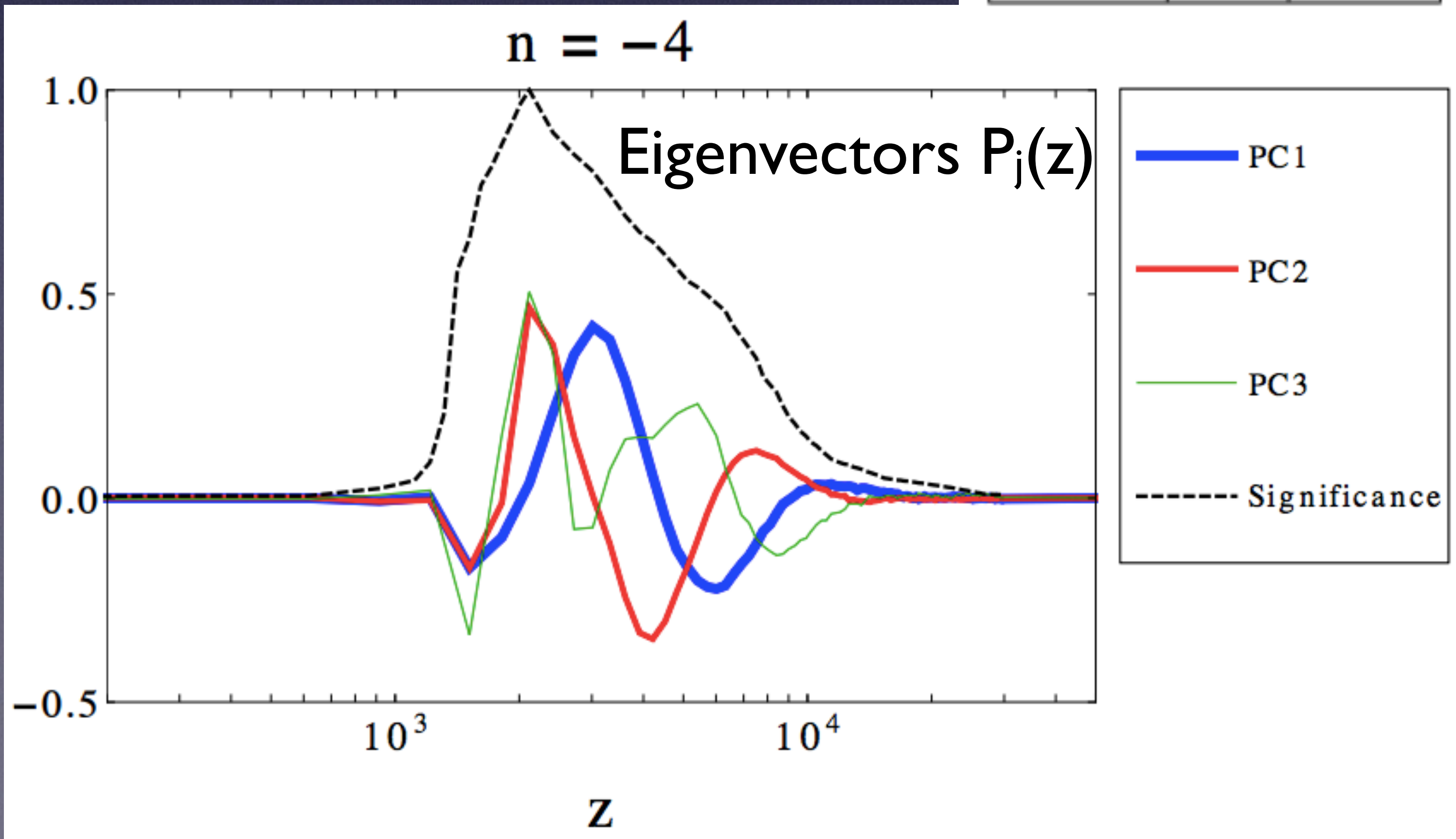

Example

- Consider simple power-law velocity dependence (for easy comparison to literature), n = -2. We will use PCs built with n=-4 baseline history.
- Convert velocity dependence to redshift dependence:
  - Assume DM thermal velocity is subdominant to baryon thermal velocity (if this is not true, linearity breaks down - more in a couple of slides!)
  - Baryon temperature set by CMB temperature.
- Now decompose new redshift-dependent cross section into principal components using α_{ij} coefficients.
- Estimate significance from eigenvalues + reading off coefficients of PCs; get constraint by demanding 2σ or smaller signal.

$$v^n \to c_n \left(\frac{T_b}{m_H} + \frac{V_{\rm rms}^2}{3}\right)^{(n+1)/2} = c_n \left(\frac{T_{\rm CMB,0}(1+z)}{m_H} + \frac{V_{\rm rms}^2}{3}\right)^{(n+1)/2}.$$

$$\sigma(z) \approx \sum_j \left[P_j(z)\sigma_0 c_n \left(\frac{T_{\rm CMB,0}(1+z)}{m_H} + \frac{V_{\rm rms}^2}{3}\right)^{(n+1)/2}\right] \times \sum_i \alpha_{ij} \frac{\sigma(z_i)}{\sigma_0 c_n \left(\frac{T_{\rm CMB,0}(1+z_i)}{m_H} + \frac{V_{\rm rms}^2}{3}\right)^{(n+1)/2}}. \quad \text{(A3)}$$

$$\sqrt{\sum_j \lambda_j \left(\sum_i \alpha_{ij} \frac{\sigma(z_i)}{c_n \left(\frac{T_{\rm CMB,0}(1+z)}{m_H} + \frac{V_{\rm rms}^2}{3}\right)^{(n+1)/2}}\right)^2} < 2.$$

$$\sigma_{-2,0} < \frac{2\sigma_0 c_n / c_{-2}}{\sqrt{\sum_{j=1}^4 \lambda_j \left(\sum_i \alpha_{ij}\left(\frac{T_{\rm CMB,0}(1+z_i)}{m_H} + \frac{V_{\rm rms}^2}{3}\right)^{-1-n/2}\right)^2}} \lesssim 1.3 \times 10^{-33}\ {\rm cm}^2$$

for n=-4

A mass-based principal component analysis for DM-baryon scattering

- Can instead test a set of basis cases with different DM masses, but fixed scattering rate history.
- In this case first PC dominates (>95% of variance), especially in n=-4 case (>99.9%).

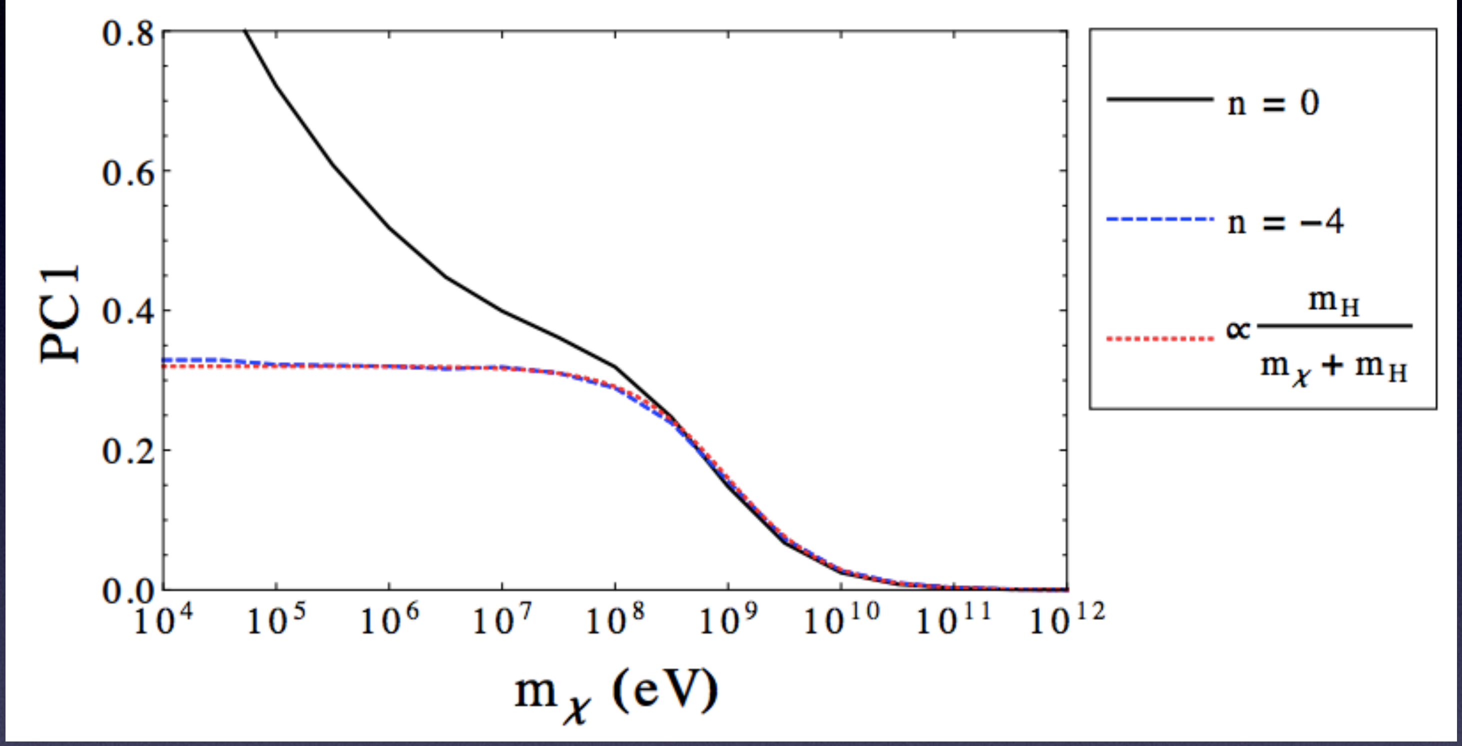

- In n=-4 case, and for n=0 at high masses, first PC (and hence detectability) scales as: $\mu/m_\chi = m_H/(m_\chi + m_H)$
- Simple explanation [Xu et al '18]: momentum transfer per scattering scales with reduced mass, scattering rate (per baryon) with DM number density (inversely proportional to DM mass).
- Breaks down for n=0 at low masses due to non-linearity effects.

Caveats

- Answer depends on how close your new history is to “baseline” - if it is far away, more PCs will be needed to capture full variance.
- Linearity will break down and this approach will fail if the DM becomes too warm - if thermal velocity from scattering-induced heating becomes comparable to baryon thermal velocity.
- Once this happens, past scattering rate → DM-baryon relative velocity → present scattering rate.
- Weakens limits for n=0 case once DM is sufficiently lighter than baryons (below ~100 MeV) - similar behavior expected for n ≥ -2.
- Irrelevant for n=-4 case as DM-baryons are never coupled in early universe with this scaling - DM can stay very cold.

Test: results of Fisher matrix vs MCMC analysis for n=-4

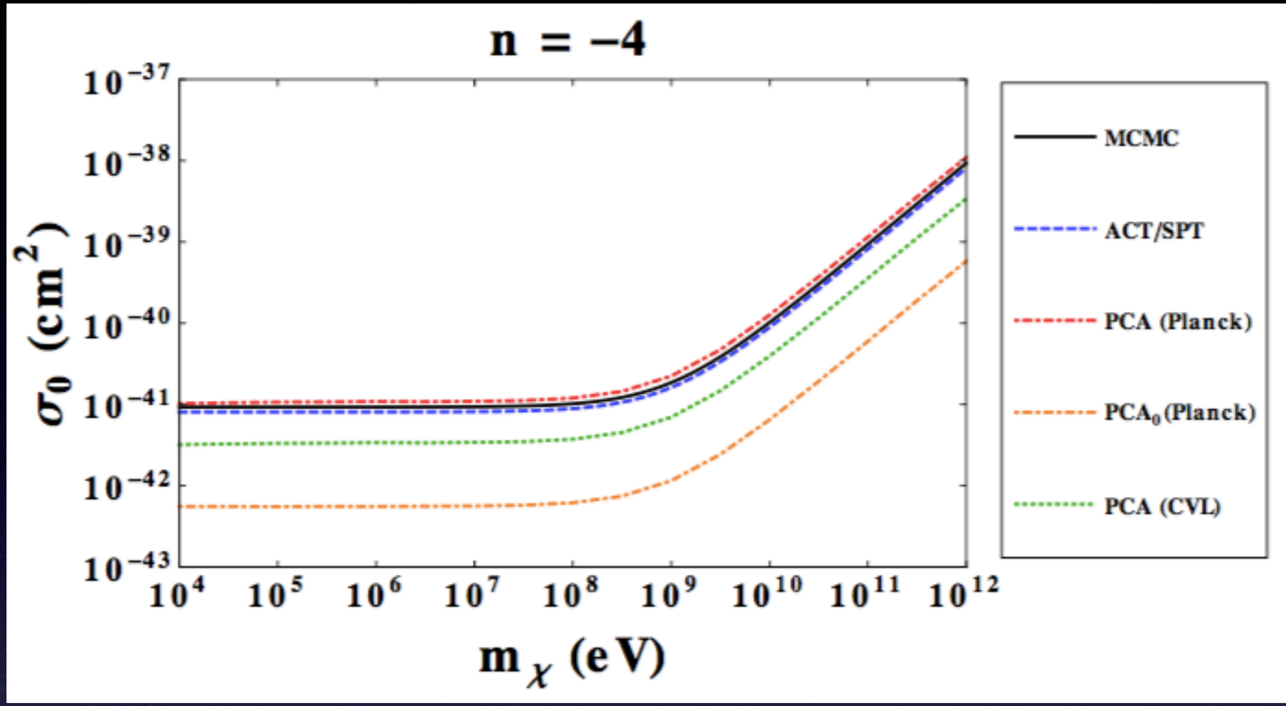

Test: results of Fisher matrix vs MCMC analysis for n=0

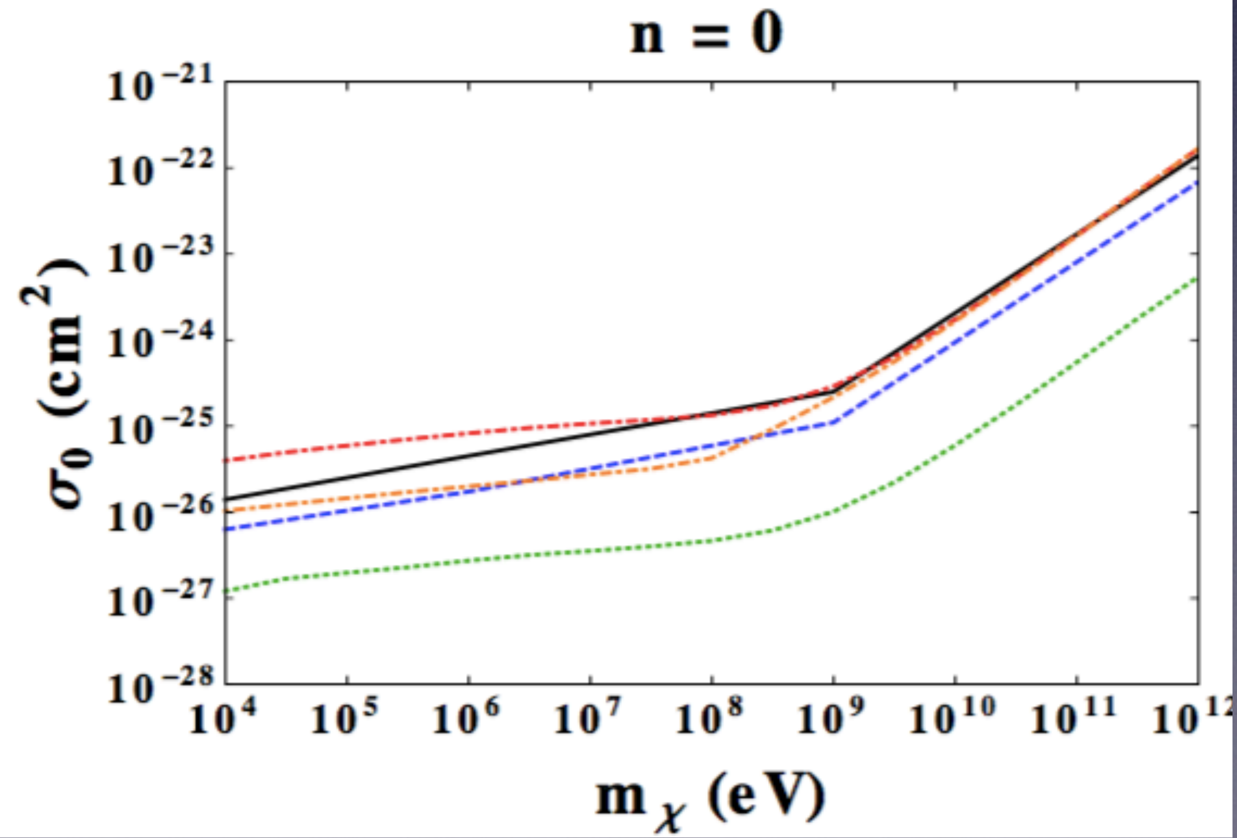

Late-time temperature

- Can keep solving for baryon temperature forward to times well after recombination.
- Once baryon and photon temperatures decouple at z~200, energy required to heat baryons is greatly reduced.
- Low velocities at late times lead to greatly enhanced effects for negative n.
- Note: again correct treatment of bulk relative velocity matters; we show results here with the mean-field treatment, but also show the effects of consistently neglecting the bulk velocity.

Temperature history for baryons and DM, CMB limits saturated, 0.1 GeV DM mass

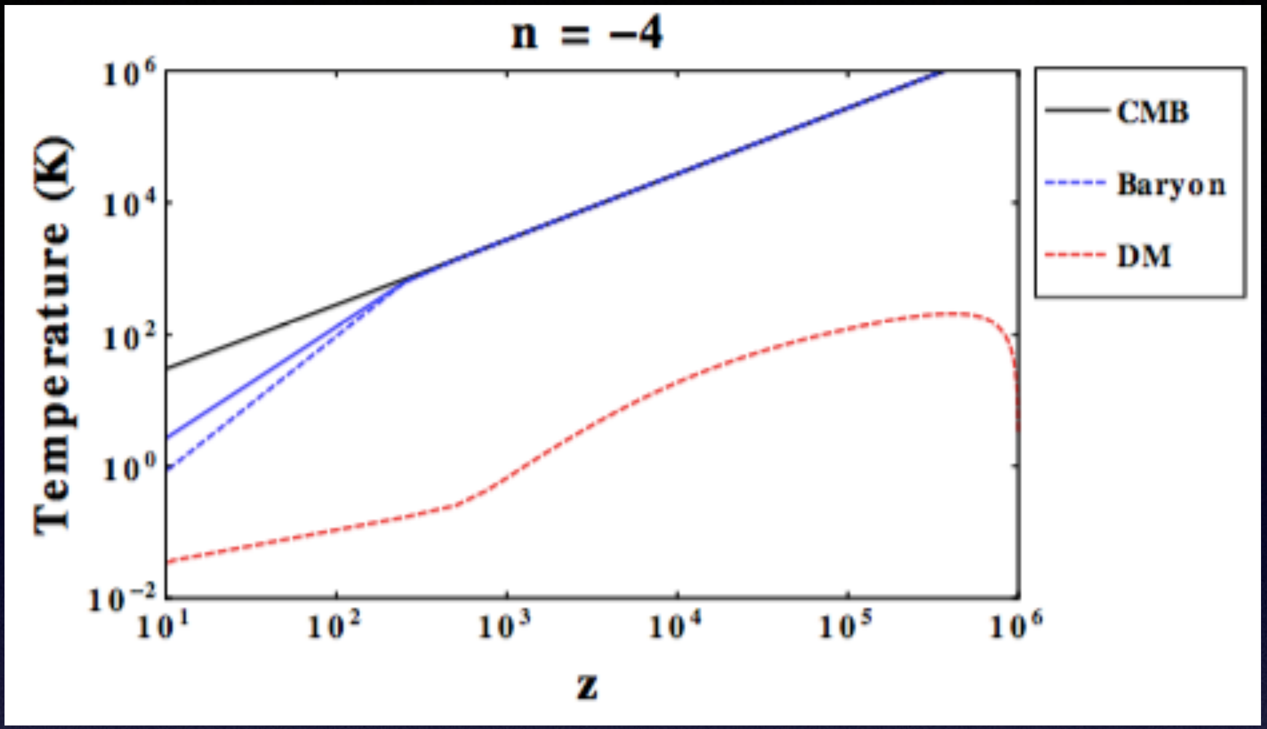

Temperature history, with saturated CMB limits, for varying n and mass (pink = 1+ GeV, red = below 1 GeV, purple = below 1 GeV neglecting v_{rms})

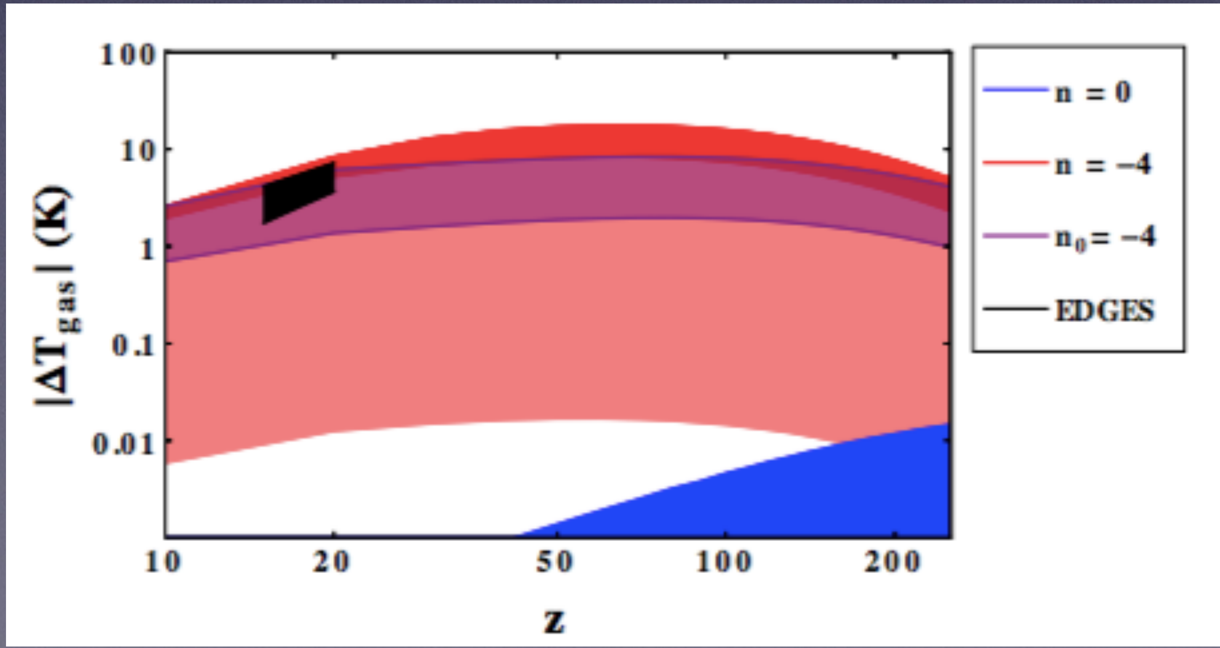

Parametrics of a 21cm signal

$$T_{21}(z) \approx x_{\rm HI}(z) \left(\frac{0.15}{\Omega_m}\right)^{1/2} \left(\frac{\Omega_b h}{0.02}\right) \times \left(\frac{1+z}{10}\right)^{1/2} \left[1 - \frac{T_R(z)}{T_S(z)}\right] 23\,\mathrm{mK},$$

- Spin-flip transition of neutral hydrogen can be used to probe temperature and distribution of the neutral gas in the early universe prior to reionization ($z > 7$ or so).
- 21cm absorption/emission signal strength depends on "spin temperature" T_S, measure of #H in ground vs excited state - expected to lie between gas temperature T_{gas} and CMB temperature T_{CMB}.
- Absorption signal when $T_S < T_R$ (radiation temperature), emission signal if $T_S > T_R$.
- T_R here describes # photons at 21cm wavelength - not necessarily thermally distributed.
- Expected behavior: T_{gas} decouples from T_{CMB} around redshift $z \sim 150$, subsequently satisfies $T_{gas} \sim T_{CMB}\,(1+z)/(1+z)_{dec}$. Gas is later heated by the stars, and eventually T_{gas} increases above T_{CMB}. Thus expect early absorption, later emission.

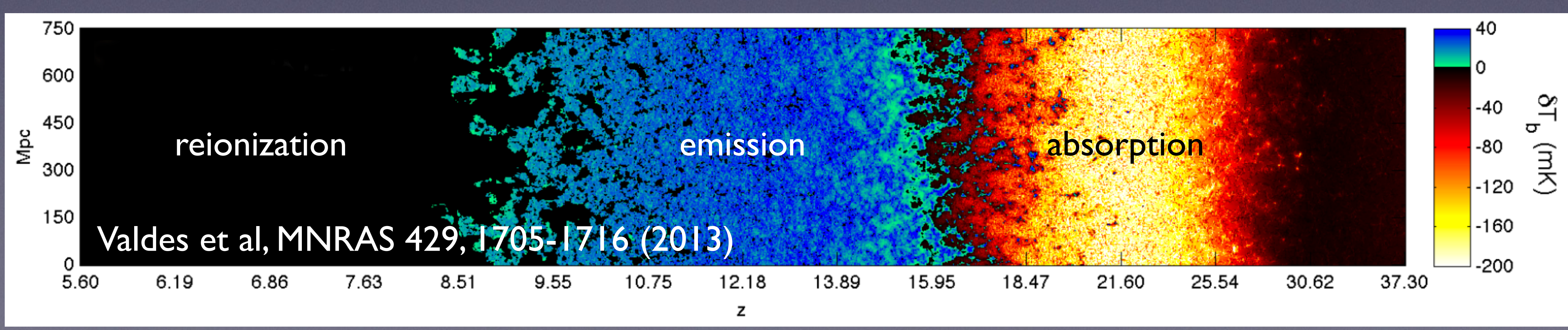

A measurement of 21cm absorption in the dark ages?

- The Experiment to Detect the Global Epoch-of-reionization Signature (EDGES) has claimed a detection of the first 21cm signal from the cosmic dark ages [Bowman et al, Nature, March '18]
- Claim is a deep absorption trough corresponding to z~15-20 - implies spin temperature < CMB temperature.
- Measurement of $T_{gas}/T_R(z=17.2) < T_S/T_R < 0.105$ (99% confidence).

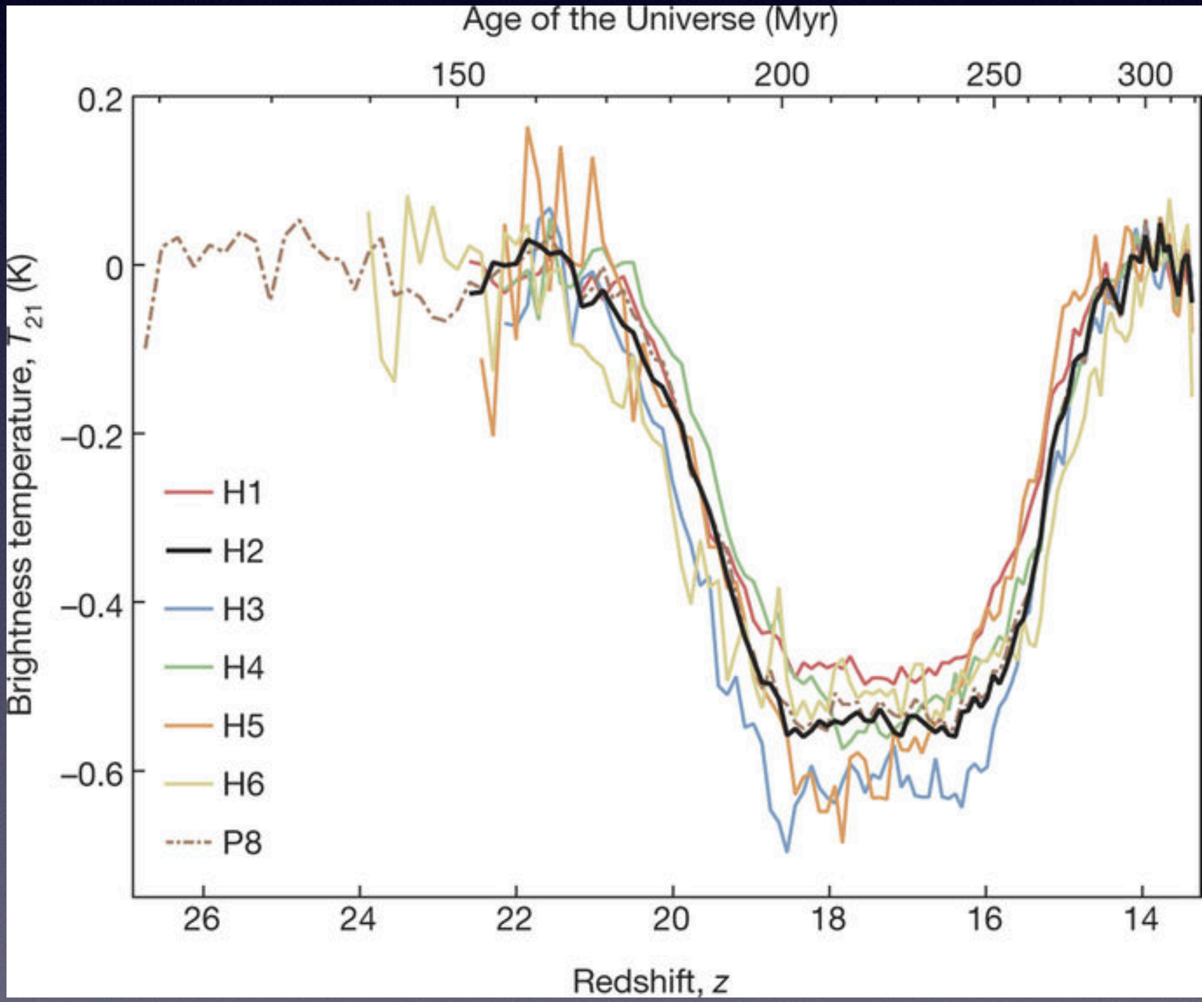

Interpreting EDGES

- If T_R is taken to be the CMB temperature, this gives $T_{gas} < 5.2$ K.
- But assuming standard decoupling and <u>no</u> stellar heating, we can calculate $T_{gas} \sim 7$ K.
- It is quite possible this result is spurious - e.g. due to instrumental effects and/or foregrounds [e.g. Hills et al 1805.01421].
- But if it is confirmed, suggests either $T_R > T_{CMB}$ (new radiation backgrounds) [Feng & Holder 1802.07432], or some modification to the standard scenario that lowers T_{gas}.
- New radiation backgrounds could arise from either novel astrophysics, i.e. radio emission from early black holes [Ewall-Wice et al 1803.01815] or more exotic (DM-related?) sources [e.g. Fraser et al 1803.03245, Pospelov et al 1803.07048].
- Additional cooling of the gas could be due to modified recombination history (earlier decoupling from CMB), or thermal contact of the gas with a colder bath, e.g. (some fraction of) the dark matter [e.g. Barkana, Nature, March '18; Munoz & Loeb 1802.10094; Berlin et al 1803.02804; Barkana et al 1803.03091; Houston et al 1805.04426; Sikivie 1805.05577].

Constraints from the CMB on the scattering interpretation

- Using our Fisher/PCA approach, we can estimate velocity scaling needed to explain EDGES if 100% of the DM is actively scattering (and CMB bounds are saturated).
- We find that in this case, sufficient cooling requires n < -3.
- This implies a long-range interaction (partial wave unitarity bound has n=-2).
- Very stringent constraints on new long-range forces (e.g. from fifth force experiments).

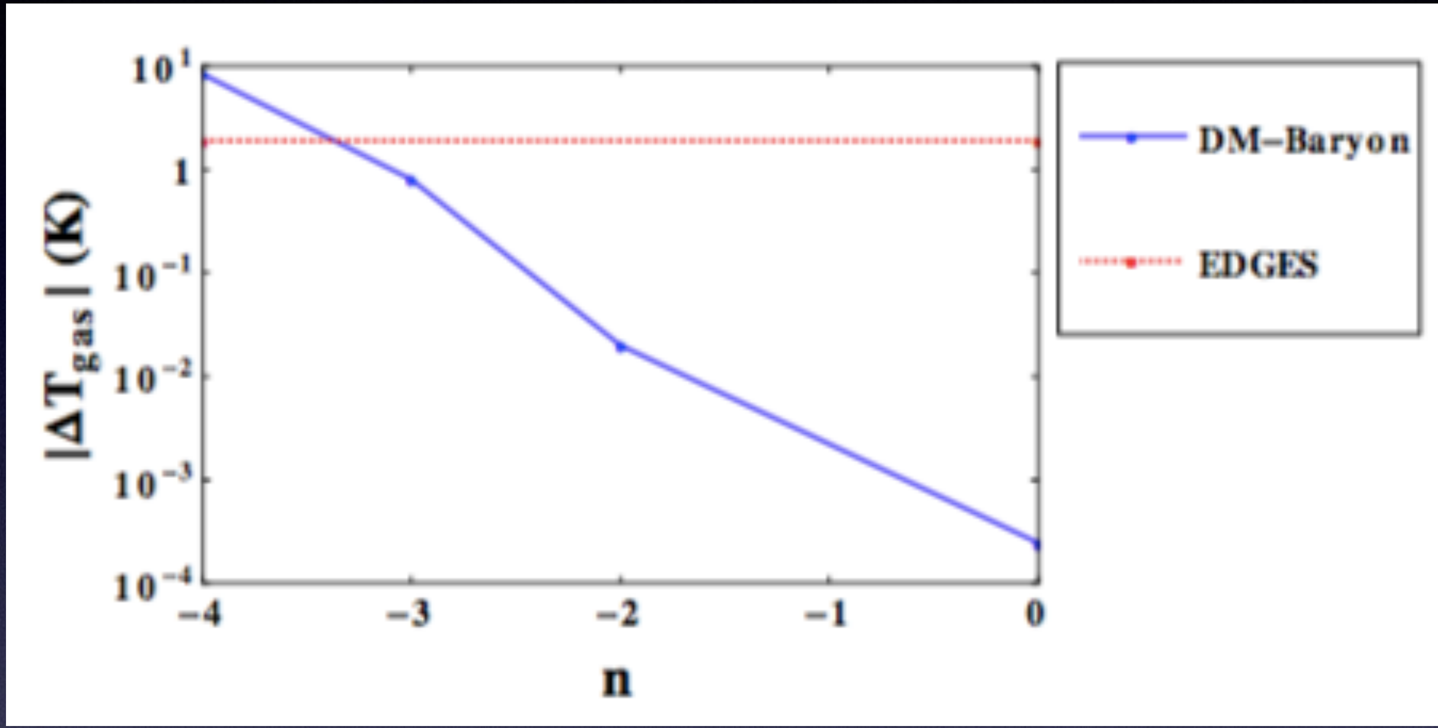

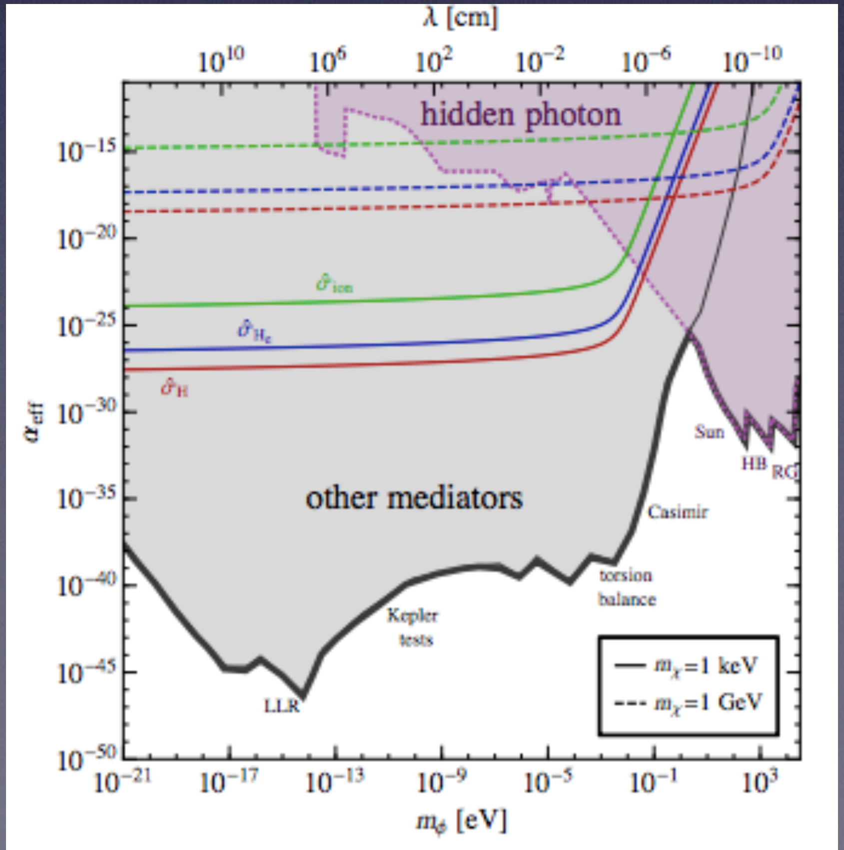

Barkana et al '18, constraints on new light mediators to generate requisite scattering

Millicharged DM?

- One possible solution: use the long-range force we know about already, let the DM carry a tiny electric charge
- Doesn't work well if 100% of the DM is charged
  - would propagate non-trivially in Galactic magnetic fields, reshaping Galactic dark matter halos
  - ionized fraction of ordinary matter is orders of magnitude smaller at z~17 than z~1000 - scattering rate for EDGES is suppressed relative to CMB limits

Kovetz et al 1807.11482

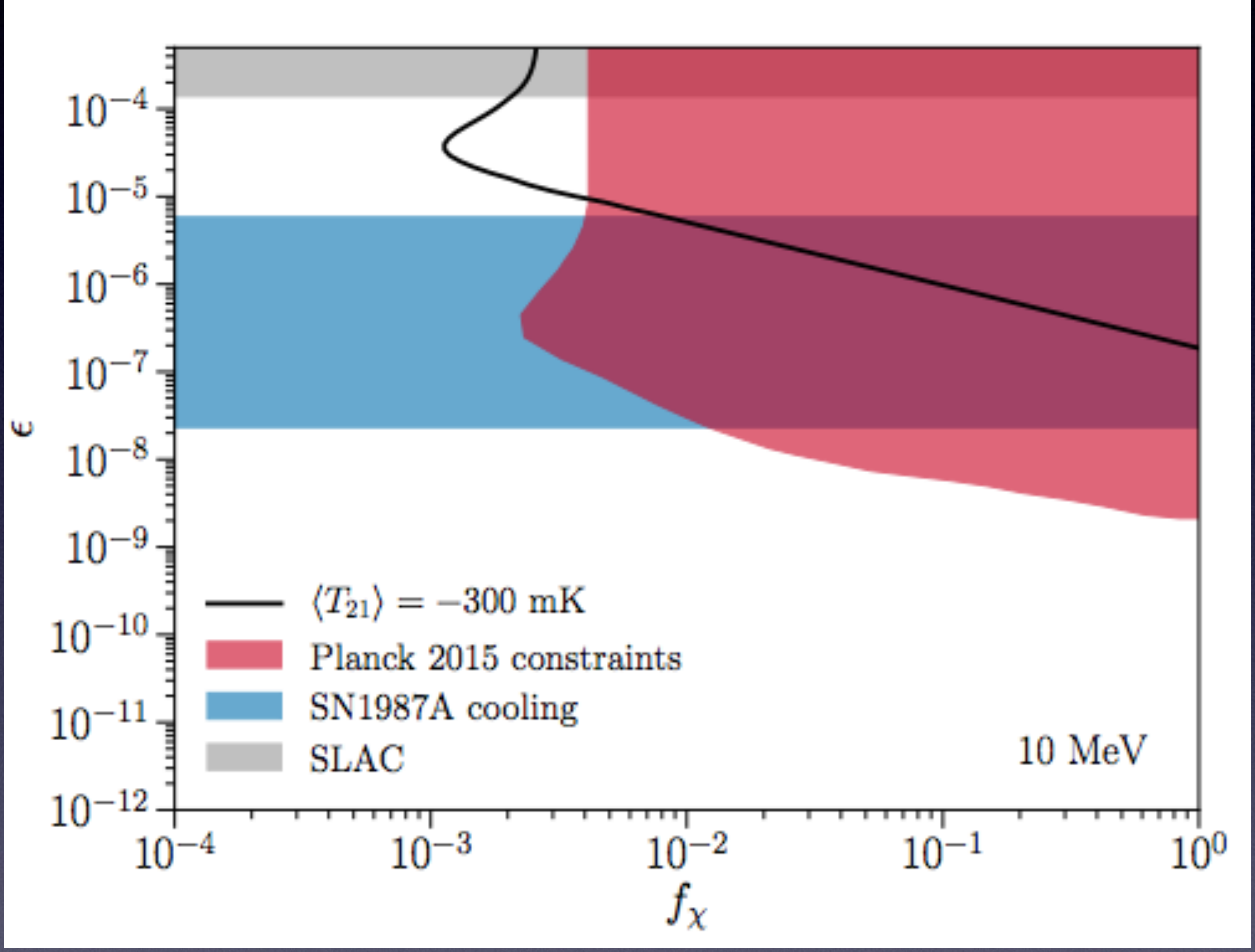

- So hypothesize that some small fraction of the DM is milli/microcharged [e.g. Munoz et al '18, Berlin et al '18, Barkana et al '18] - this also helps evade CMB bounds, as bulk of DM behaves like ordinary CDM.
- Need low mass / high number density; latest analysis finds millicharged fraction needs to be 0.01-0.4% of DM, in mass range 0.5-35 MeV [Kovetz et al '18].

Early cooling and the CMB

- CMB anisotropies are sensitive to fraction of the DM that is scattering.
- But CMB energy spectrum measures energy flow - same as EDGES, but at earlier times.
- Heating/cooling of the gas tightly coupled to the CMB at early types induces a spectral distortion [Ali-Haimoud et al ‘2015, Choi et al ’17], with the net energy flow being

$$\rho_\gamma \frac{d\Delta}{dt} = \frac{3}{2} n_b \frac{2\mu_b}{m_e} R_\gamma \left(T_b - T_\gamma\right)$$

- We integrated this distortion from $z \sim 2\times10^6 - 10^4$ for millicharged DM (with CLASS) adding up contributions to the T_b evolution from millicharged-DM scattering with protons/electrons/helium.

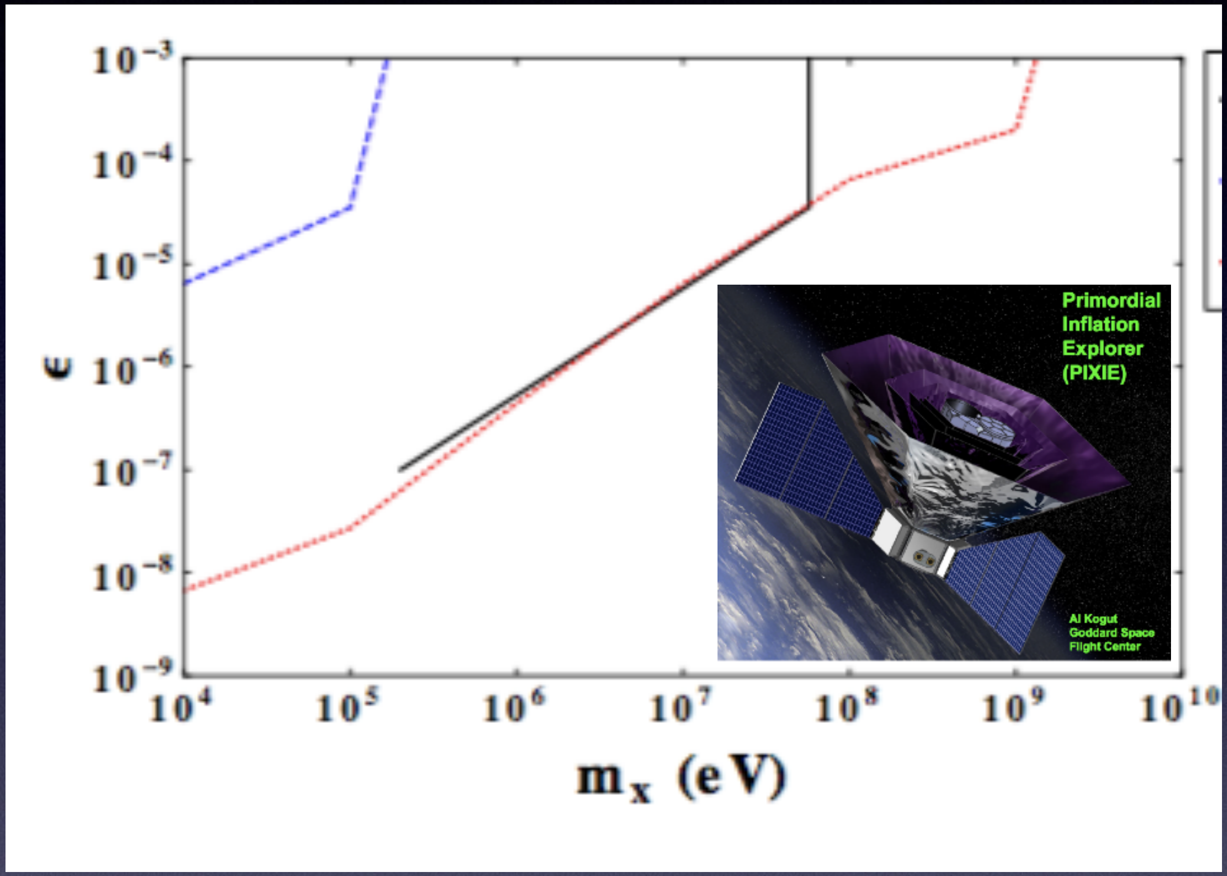

Forecast constraints for 1% of DM scattering

- We find that next-gen experiments, with sensitivity to $\sim 10^{-8}$ distortions, could test the parameter space claimed to explain EDGES.

Annihilation

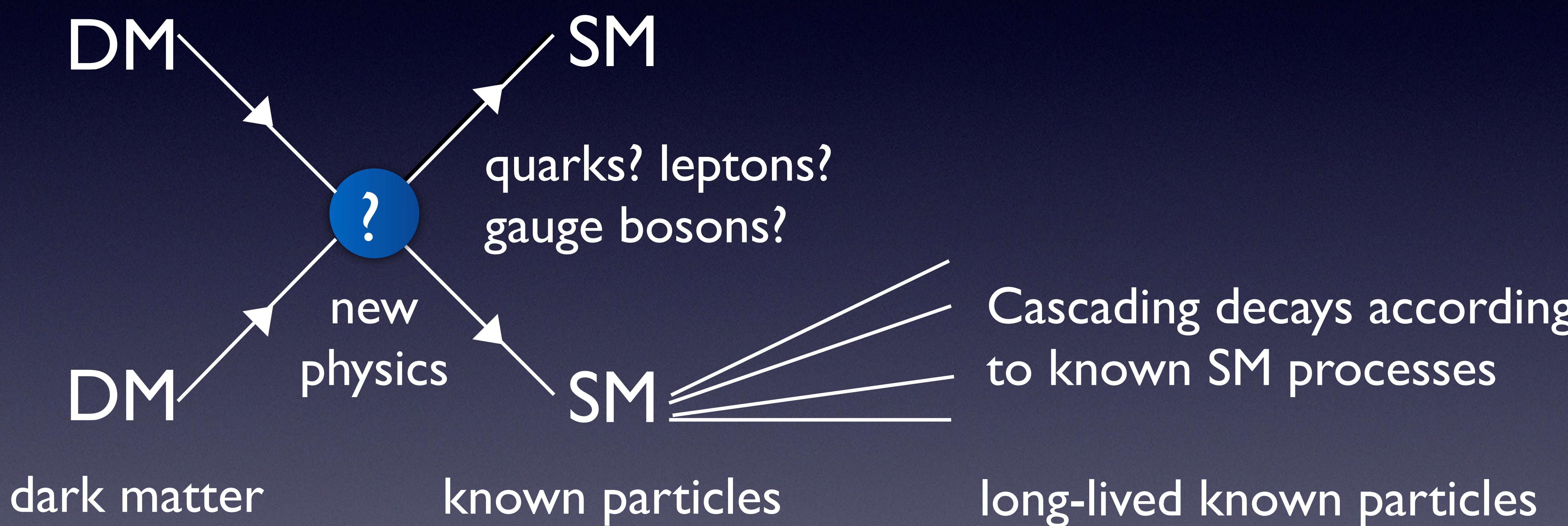

Annihilation

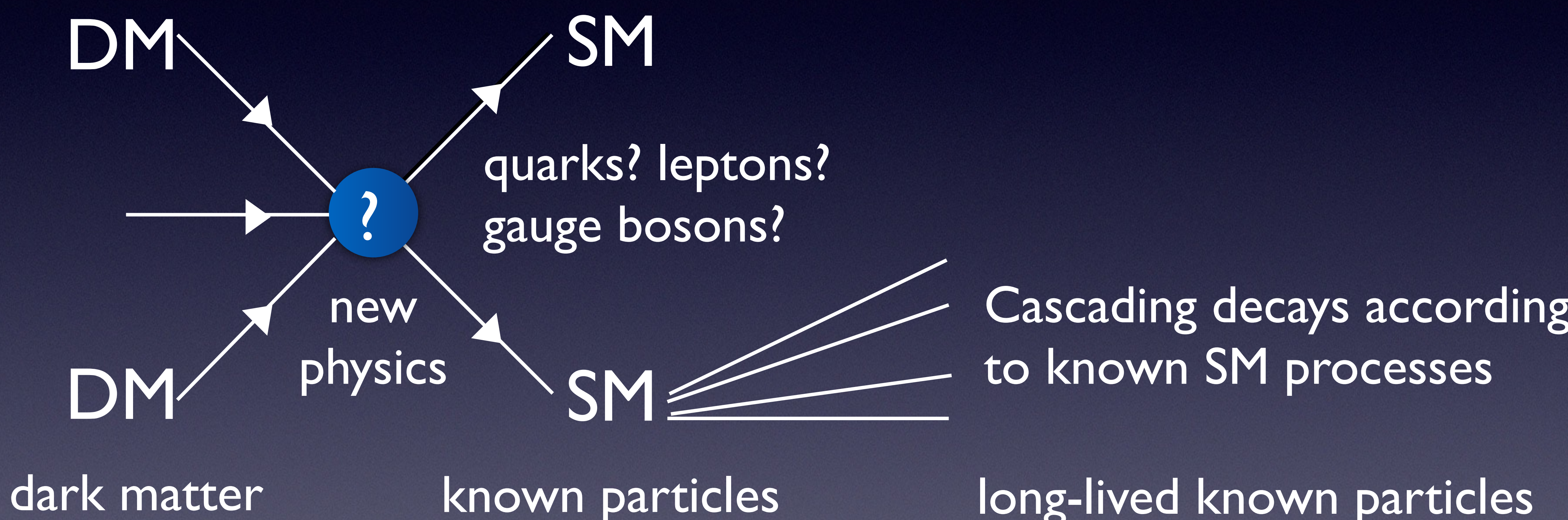

CMB annihilation bounds

- CMB anisotropy measurements place powerful limits on (2-body) DM annihilation for keV+ DM - nominally exclude thermal relic cross section for masses below ~10 GeV (if annihilation is into visible channels), often set strongest indirect limits on light DM.
- Mechanism: high-energy particles produced by annihilation cool and produce secondaries, which ionize hydrogen. Extra free electrons scatter CMB photons.
- Much interest in recent years in models where 3-body processes determine freezeout [e.g. work on SIMPs pioneered by Berkeley group, Hochberg et al ’14, ’15, ’18]: naturally low mass scale, can evade many constraints.
- Classic SIMP annihilation is entirely within dark sector - but even if SM particles are produced [as e.g. in Cline, TRS et al ’17], extra density scaling of 3-body annihilation should strongly suppress indirect signals.

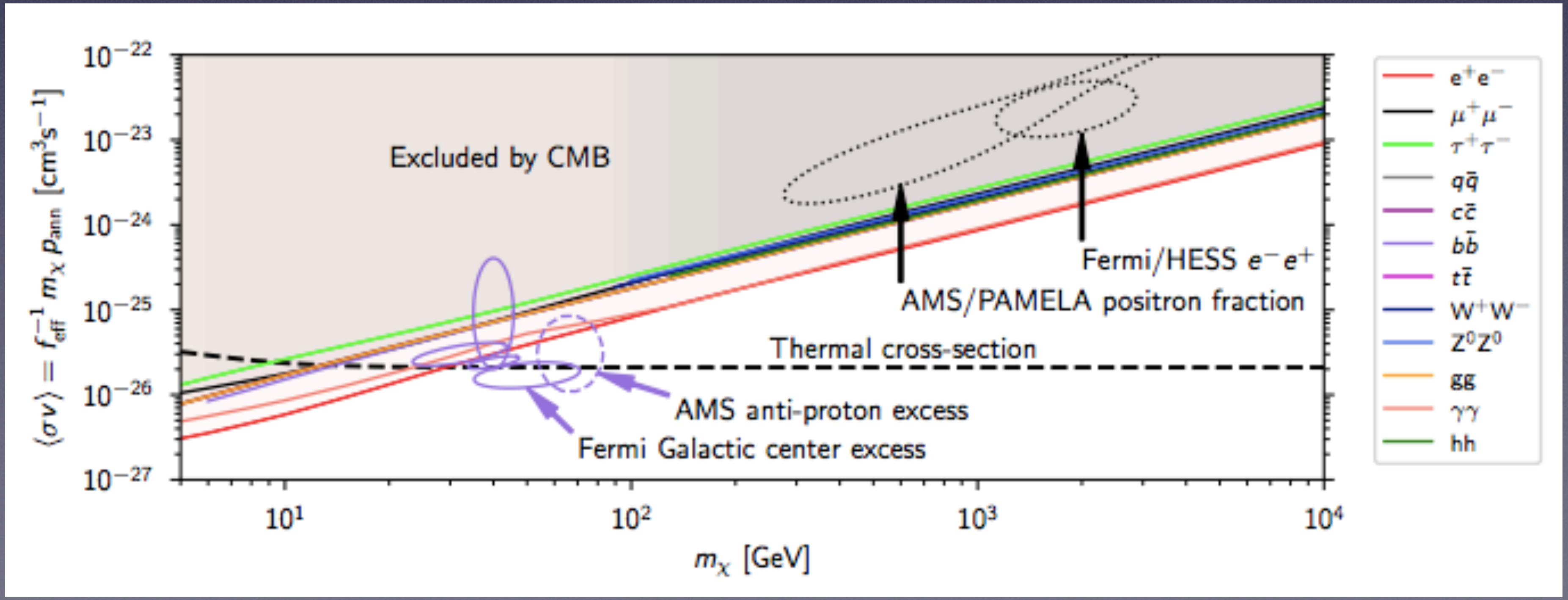

Planck Collaboration ’18 1807.06209

Back of the envelope I

- Consider the power from DM annihilation - how many hydrogen ionizations?
  - 1 GeV / 13.6 eV ~ 10^8
  - If 10^{-8} of baryonic matter were converted to energy, would be sufficient to ionize entire universe. There is ~5x as much DM mass as baryonic mass.
  - If one in a billion DM particles annihilates (or decays), enough power to ionize half the hydrogen in the universe…
  - More realistically, not all the power goes into ionization, but an O(0.1) fraction does - and we can measure changes to the ionization level of O(10^{-4}).
  - Bottom line: can constrain roughly one in 10^{11} DM particles annihilating to ionizing particles per Hubble time, during cosmic dark ages.

Back of the envelope II

- For thermal relic dark matter, what fraction of DM do we expect to annihilate per Hubble time?
    - At freezeout this quantity is O(1) by definition.
    - After freezeout but during radiation domination, fraction of DM annihilating per unit time scales as $(1+z)^3$ (for 2-body annihilation), Hubble time scales as $M_{Pl}/T^2 \propto (1+z)^{-2}$.
    - Thus fraction annihilating per Hubble time scales roughly as (1+z); expect to be able to probe freezeout occurring at $T \sim 10^{11} \times T_{recombination} \sim 100$ GeV.
    - For n-body annihilation, instead this quantity scales as $(1+z)^{3n-5}$.
    - 3-body: 11 orders of magnitude from $(1+z)^4$ scaling - can maybe test freezeout at keV scale? Scale only gets lower for higher-order processes.
- keV-scale decoupling encounters limits on warm dark matter (also issues with BBN limits on # of relativistic degrees of freedom).
- Also much lower than natural scale for 3-body thermal relic: $m_{\rm DM} \sim \alpha \sqrt[n]{M_{\rm Pl} T_{\rm eq}^{n-1}}$
- This assumes cosmological scaling of DM density though - can we do any better once structure starts to form?

Indirect signals from n-body annihilation

- First-pass estimates for sensitivity to multi-body annihilation from:
  - Cosmic microwave background
  - Observations of Galactic halo in X-ray/gamma-ray band [adapting limits from Essig et al '13]
  - X-ray observations of Galactic Center and galaxy clusters [adapting searches by NuSTAR, Chandra, etc]
- Results are extremely sensitive to density profile / amount of small-scale substructure - we tested a wide range of possibilities (some of which are almost certainly too optimistic)

$$\xi \equiv (dE/dV/dt)/\rho_{\rm DM}^n \sim \langle \sigma v^2 \rangle / m_\chi^2 (n=3)$$

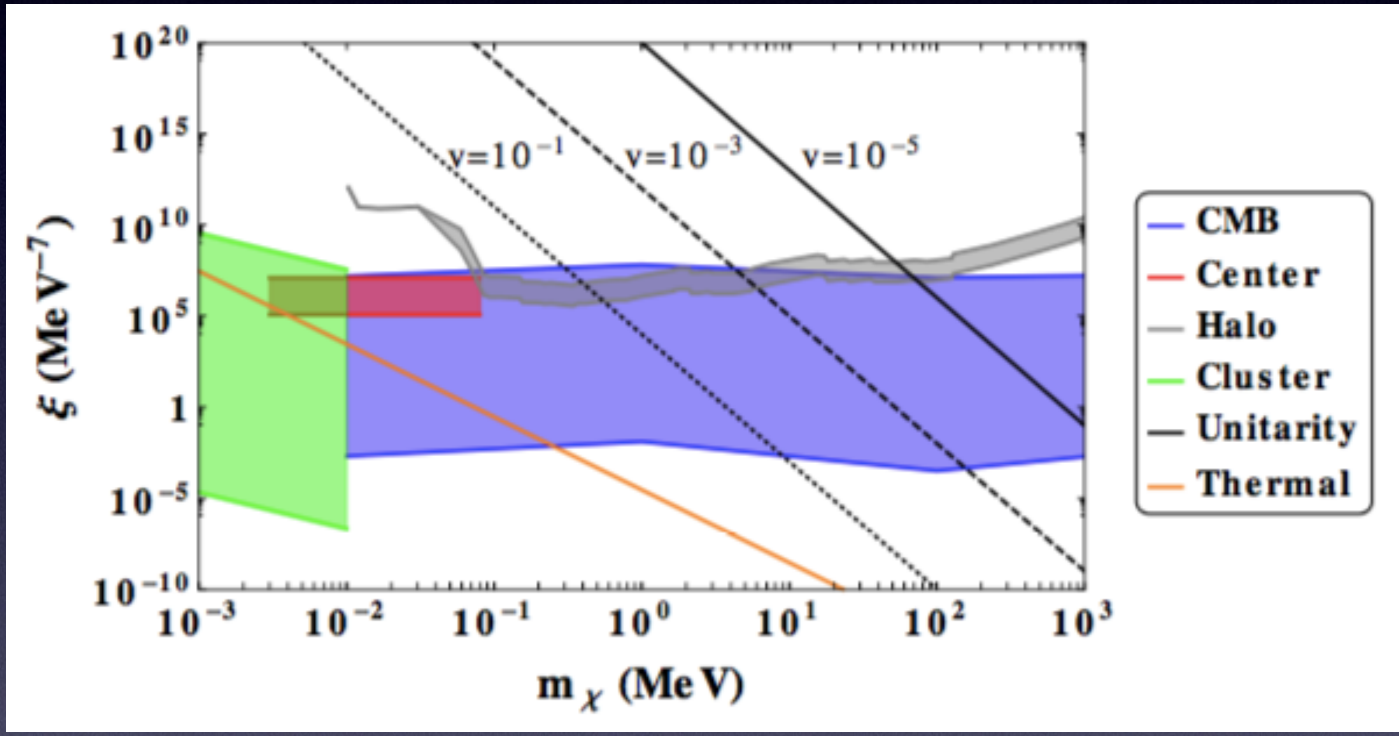

- Bottom line: in (very) optimistic substructure models, could potentially see 3-body annihilation products from generic thermal relics in the CMB (below ~100 keV) or X-ray observations of clusters (below ~10 keV).
- Robust/conservative limits do not constrain the generic thermal parameter space at all.

A note on CMB limits

- For 2-body annihilation, high redshifts (z~600) dominate the CMB signal, even with very optimistic prescriptions for structure formation.
- This is *almost* still true for 3-body annihilation - the epoch of structure formation can dominate, but only for very optimistic structure formation models (concentration growing as a power-law for very small halos, and a low minimum halo mass).
- For 4-body annihilation, the high-redshift signal can be swamped by low redshifts even for more modest amounts of substructure.

"Weighting functions" for CMB signals, for different substructure models

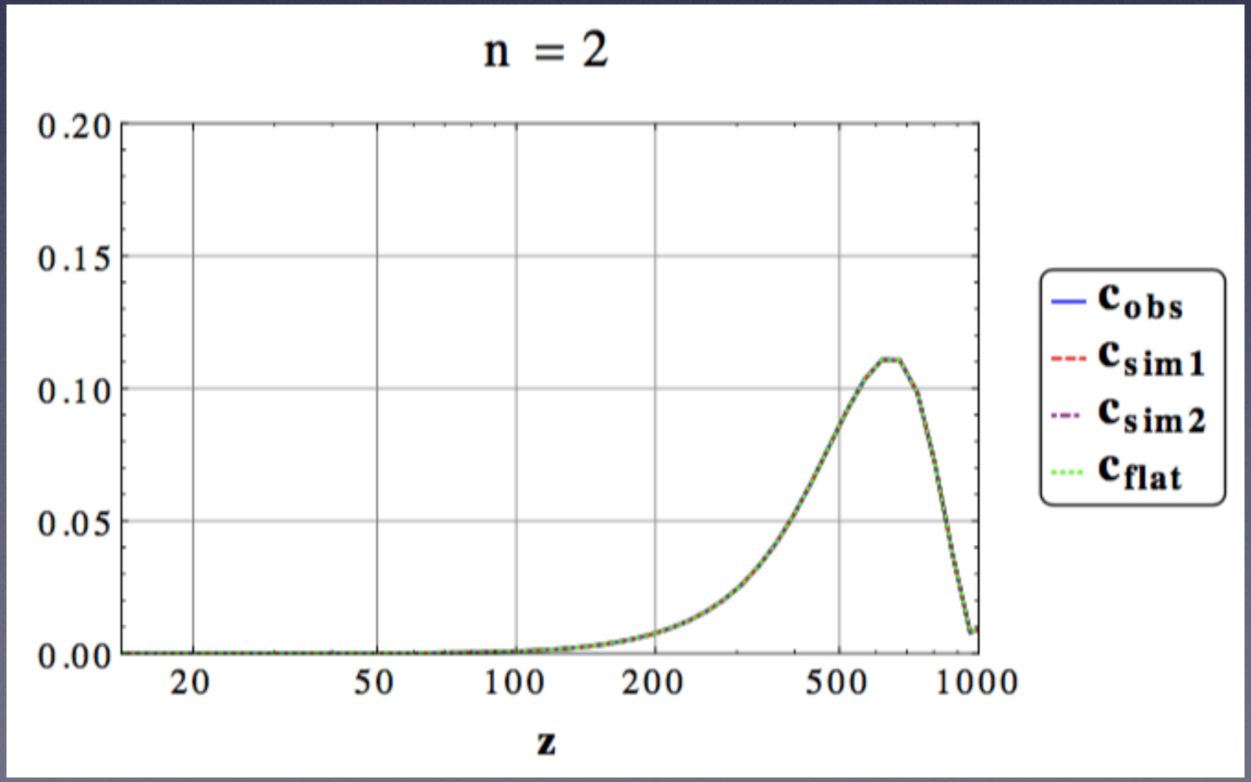

A note on CMB limits

- For 2-body annihilation, high redshifts (z~600) dominate the CMB signal, even with very optimistic prescriptions for structure formation.
- This is *almost* still true for 3-body annihilation - the epoch of structure formation can dominate, but only for very optimistic structure formation models (concentration growing as a power-law for very small halos, and a low minimum halo mass).
- For 4-body annihilation, the high-redshift signal can be swamped by low redshifts even for more modest amounts of substructure.

“Weighting functions” for CMB signals, for different substructure models

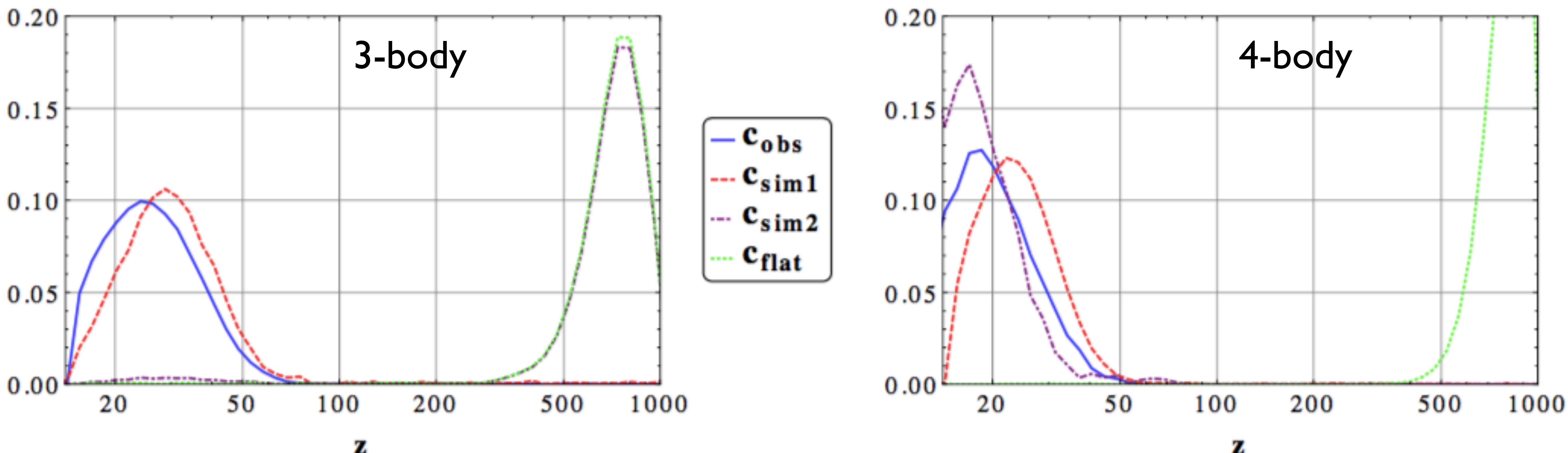

Hope for a visible signal?

- Option 1: spike in the power spectrum leading to a population of ultracompact minihaloes - could potentially affect CMB or produce visible X-ray or gamma-ray point sources.
- For benchmark thermal-relic models we tested in tens-100s of MeV range, a visible signal would require more than ~0.1% of DM to be collapsed into such objects.
- Note: recent work has also questioned whether such minihaloes can form and be stable in CDM cosmology [e.g. Gosenca et al '18, Delos et al '18].

Hope for a visible signal?

- Option 2: annihilation rate could scale with parameters other than density.
- Simple example: low-velocity enhancement.
- 2-body case: Breit-Wigner enhancement [e.g. Ibe et al '09] or Sommerfeld enhancement [e.g. Hisano et al '05] can enhance cross sections at low velocities, up to unitarity bound

  $\sigma_{\text{s-wave}} \lesssim 4\pi/k^2$

- It turns out [e.g. Mehta et al '09] that for n-body annihilation, the partial-wave-unitarity-saturating rate coefficient (equivalent of σv) scales as $1/v^{3n-5}$

Implications of low-velocity enhancements

- In cosmology, after the DM fully decouples from the SM, its velocity scales as v ~ (1+z), whereas density scales as $(1+z)^3$.
- Consequently the overall n-body annihilation rate (per volume per time), in the unitarity limit, would scale as density^n velocity^{5-3n} ~ $(1+z)^5$.
- Thus independent of n, <u>all</u> unitarity-saturating cross sections scale in the same way with redshift, after decoupling and prior to structure formation.
- In this limit, we should expect CMB signals from multi-body annihilation similar to Sommerfeld-enhanced two-body annihilation.
- With the onset of structure formation, density and velocity are decoupled - multi-body signals in unitarity regime would favor high-density, low-velocity objects (i.e. substructure even <u>more</u> important).

Implications of low-velocity enhancements

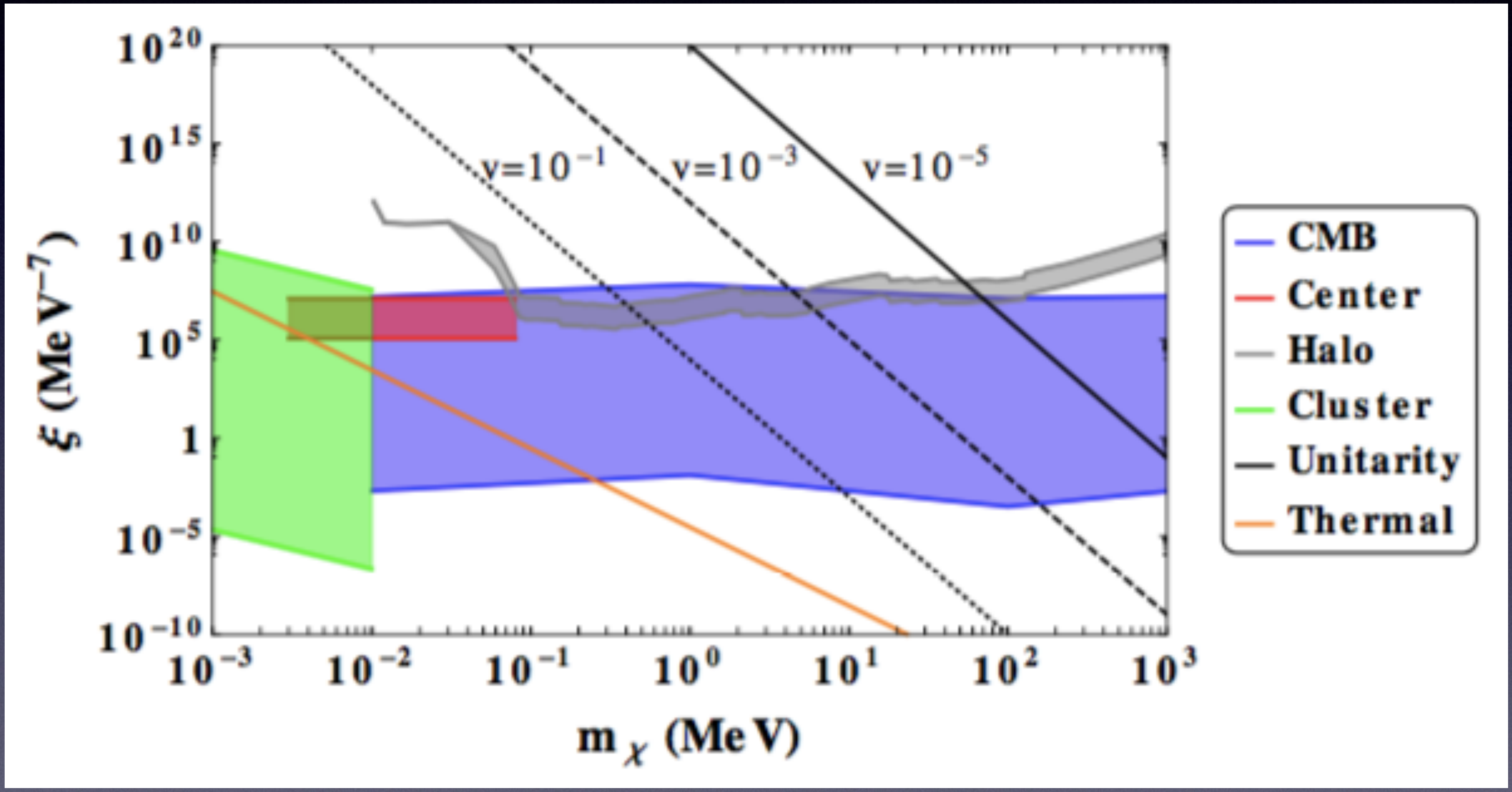

- Example: the robust CMB bound can test unitarity-saturating cross sections for masses below ~100 MeV, even if the DM velocity after recombination is ~10^{-5}, comparable to the baryon velocity (to put it another way, at masses well above 100 MeV, the CMB cannot robustly test even the unitarity-saturating cross section unless the DM velocity is substantially below 10^{-5}).

Example of a model with low-velocity enhancement

- "Not forbidden dark matter" [Cline, TRS et al '17] - dark sector contains massive dark photon (A') + fermionic dark matter (χ).
- 3-body semi-annihilation can control freezeout process if $m_\chi < m_{A'} < 2m_\chi$.
- Resonant enhancement occurs in non-relativistic limit as $m_{A'} \to 2m_\chi$ from below.

$$\chi\chi\bar{\chi} \to \chi A'$$

$$\frac{1}{(k_1+k_2)^2 - m_{A'}^2} \to \frac{1}{(2m_\chi)^2 - m_{A'}^2}$$

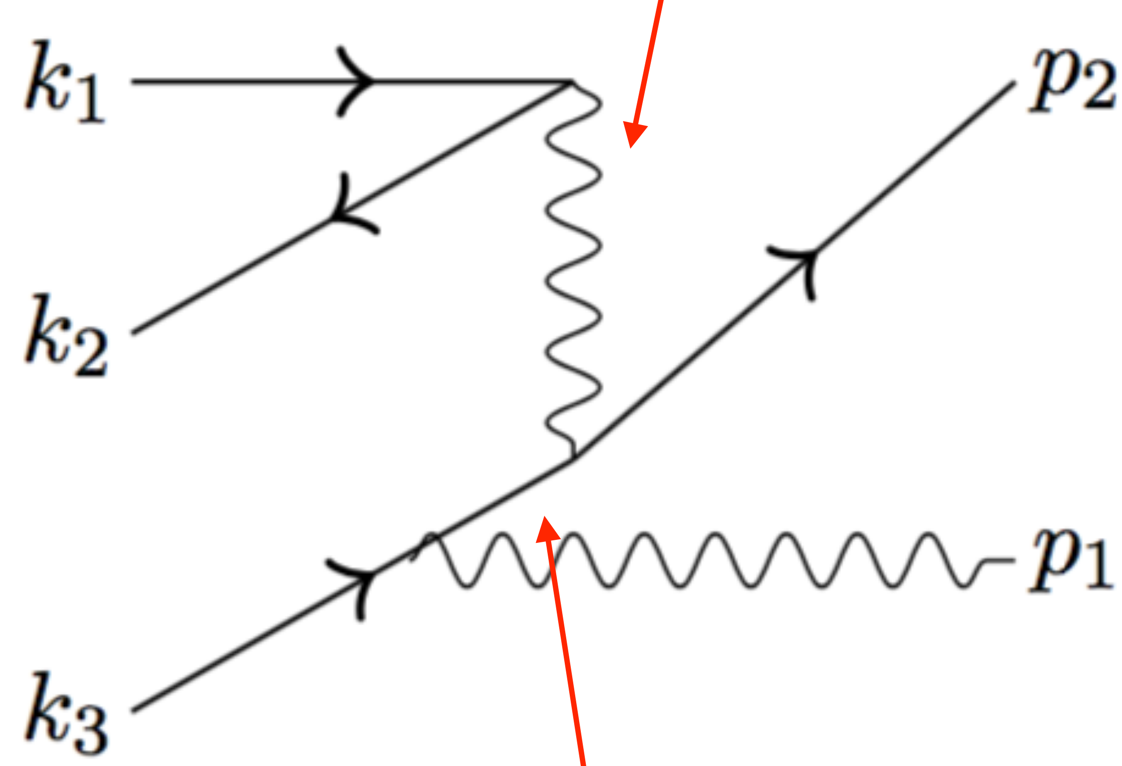

$$\frac{1}{(k_3-p_1)^2 - m_\chi^2} \to \frac{1}{(m_\chi - m_{A'})^2 - m_\chi^2}$$

Summary

- Measurements of the CMB anisotropies set stringent constraints on the scattering cross section between (the bulk of the) dark matter and visible matter, at redshifts $10^{3\text{-}4}$. I have presented a framework for estimating the CMB constraint on arbitrary redshift-dependent scattering histories.
- The claimed EDGES result could indicate a colder-than-expected gas temperature at $z\sim17$; this in turn might be a hint of DM-baryon scattering. However, if 100% of the DM scatters, the cross section must be strongly enhanced at low temperatures to evade CMB bounds.
- These bounds can be escaped if only a small fraction (<0.4%) of the DM scatters with the CMB. Future measurements of the CMB energy spectrum could test the hypothesis that a small fraction of DM carries tiny electric charge and is responsible for the EDGES signal.

- Annihilation processes with more than two DM particles in the initial state are very challenging to see in indirect detection; my collaborators and I have mapped current limits onto the 3-body case, and shown that there are no robust constraints on the parameter space for generic thermal relics from 3-body annihilation.
- However, Standard Model particles produced in such processes may be visible if, for example:
  - the DM mass scale is sufficiently low (sub-MeV) and there is a very large amount of small-scale substructure.
  - a substantial fraction (>0.1%) of the DM is collapsed into ultracompact minihalos.
  - the annihilation rate is enhanced at low velocities. In this last case, partial-wave unitarity permits a much stronger scaling with velocity for multi-body processes. This could potentially lead to highly-enhanced signals at low redshifts, especially in regions of high density and low velocity.